Polycaprolactone Nanoparticle Encapsulating Antifouling Ceftaroline for Enhanced In-vitro Controlled Drug Release

Author

Naeema Hanif

Regn Number

00000363583

Supervisor

Dr. M. Nabeel Anwar

DEPARTMENT OF BIOMEDICAL ENGINEERING & SCIENCES (BMES)

SCHOOL OF MECHANICAL & MANUFACTURING ENGINEERING (SMME)

NATIONAL UNIVERSITY OF SCIENCES AND TECHNOLOGY

ISLAMABAD (NUST)

JANUARY 2024

Polycaprolactone Nanoparticle Encapsulating Antifouling Ceftaroline for Enhanced In-vitro Controlled Drug Release

Author

Naeema Hanif

Regn Number

00000363583

A thesis submitted in partial fulfillment of the requirements for the degree of

MS Biomedical science

Thesis Supervisor:

Dr. M. Nabeel Anwar

Thesis Supervisor's Signature: _____

DEPARTMENT OF BIOMEDICAL ENGINEERING & SCIENCES (BMES)

SCHOOL OF MECHANICAL & MANUFACTURING ENGINEERING(SMME)

NATIONAL UNIVERSITY OF SCIENCES AND TECHNOLOGY(NUST),

ISLAMABAD

JANUARY, 2024

THESIS ACCEPTANCE CERTIFICATE

Certified that final copy of MS/MPhil thesis written by **Regn No. 00000363583 Naeema Hanif** of **School of Mechanical & Manufacturing Engineering (SMME)** has been vetted by undersigned, found complete in all respects as per NUST Statues/Regulations, is free of plagiarism, errors, and mistakes and is accepted as partial fulfillment for award of MS/MPhil degree. It is further certified that necessary amendments as pointed out by GEC members of the scholar have also been incorporated in the said thesis titled. **Polycaprolactone Nanoparticle Encapsulating Antifouling Ceftaroline for Enhanced In-vitro Controlled Drug Release**

Signature:

Name (Supervisor): Muhammad Nabeel Anwar

Date: 24 - Jan - 2024

Signature (HOD):

Date: 24 - Jan - 2024

Signature (DEAN):

Date: 24 - Jan - 2024

DECLARATION

I certify that this research work titled **"Polycaprolactone Nanoparticle Encapsulating Antifouling Ceftaroline for Enhanced In-vitro Controlled Drug Release"** is my own work. The work has not been presented elsewhere for assessment. The material that has been used from other sources has been properly acknowledged / referred.

Signature of Student

Naeema Hanif

2021-NUST-MS-BMES-00000363583

COPYRIGHT STATEMENT

ACKNOWLEDGEMENTS

Dedicated to my exceptional parents and adored siblings whose tremendous support and cooperation led me to this wonderful accomplishment.

ABSTRACT

Globally, infectious diseases are among the top ten significant contributors to large number of fatalities affecting both developed and developing countries evenly. It has been challenging to treat infections like skin infections due to the global trend of developing antibiotic resistance. In context of this, antibiotics that are effective against both gram-positive and gram-negative organisms and have a long half-life as well as high tissue permeability are needed. Cefepime, a member of the fourth generation intravenous cephalosporins, is one such antibiotic. However, the intravenous administration of drug has restricted the supply of drug to the intended area i.e., skin, instead reaches directly to the blood. This draws attention to the significance of developing a drug delivery system that stays at the skin surface while regulating drug absorption, boosts the drug's bioavailability, and lessens the requirement for frequent drug usage. The current research focuses on developing a chitosan nano-carrier using the ionic gelation method, subsequently transformed into carbopol gel for more effective, longer-lasting skin drug release. SEM analysis shows the spherical morphology of chitosan/alginate nanoparticles with sizes of 156 ± 12.75nm and 222 ± 56nm for both blank and drug-loaded nanoparticles, respectively. Positive zetapotential i.e., 18.2mV indicates polycationic chitosan matrix of the nano-capsules. Finally, the in-vitro drug release study manifested controlled drug release at two different pH (5.5 and 7.4) for a period of 24h. Furthermore, antibacterial activity of nano-formulation as well as the gel was observed against both +Ve and -Ve bacterial strains with better zones of inhibition. The obtained data significantly pointed out that the cefepime nanoparticles loaded carbopol gel would be an encouraging choice for skin infections.

Key words

Topical drug delivery; polymeric nanoparticles; drug resistance; cefepime HCL; ionic gelation method; chitosan; sodium alginate; carbopol 940; gram positive and negative bacterial strains; skin infections.

TABLE OF CONTENTS

LIST OF FIGURES

LIST OF TABLES

LIST OF ACRONYMS

Acronym	Full Form
CHN	Chitosan
Na-ALG	Sodium Alginate
NPs	Nanoparticles
CEF-HCL	Cefepime Hydrochloride
PDI	Poly-dispersity index
SEM	Scanning-electron microscopy
XRD	X-ray Diffraction
FTIR	Fourier Transform infrared spectroscopy
EE	Entrapment Efficiency
PBS	Phosphate buffer solution
MHA	Mueller Hinton Agar

Graphical abstract
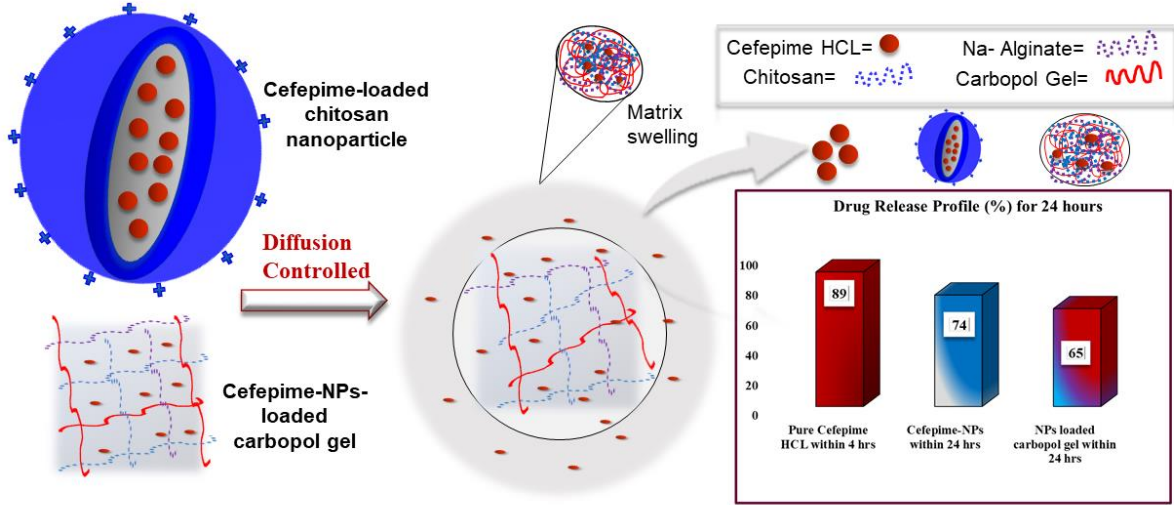
CHAPTER 1. INTRODUCTION

1.1. Background

In the past, infectious diseases have been a leading cause of death. However, advancements in public health and medicine during the 20th century significantly lessened the burden brought on by infectious illnesses. In 1900, out of the top 10 primary causes of mortality, infectious diseases were responsible for one-third of all fatalities (Diseases).On the other hand, noncommunicable disorders including cancer and cardiovascular disease caused the bulk of deaths in 2014(Nichols 2018). Major medical advances, like the discovery of penicillin and cephalosporin, as well as better sanitation, were essential in lowering the mortality rate related to infections (Nichols 2018). Since antibiotic-resistant infections impact both industrialized and developing nations equally, it is crucial to examine the worldwide trend of antibiotic resistance. Although it is challenging to obtain precise estimates of drug resistance, it is anticipated that if the right steps are not taken, antimicrobial-resistant diseases will result in almost 10 million deaths annually by 2050 and a total GDP loss of $100.2 trillion (Nichols 2018).

1.2. Bacterial skin infections

The primary source of skin and skin-structure infections is trauma or a rupture in the natural skin barrier, which permits bacteria to enter the subcutaneous region. These ruptures are frequently vulnerable to surface contamination, and Staphylococcus aureus or streptococci are frequently the culprits causing illnesses (Swartz 2000).

Drug resistance to multiple medications that require frequent dosage and may cause missed doses make it difficult to treat complicated mixed infections of the skin and skin structure. A prolonged lifespan, significant tissue permeability, and efficacy against both gram-negative and gram-positive organisms represent the desirable properties of an antibiotic (Kessler, Bies et al. 1985).

Cefepime is a fourth-generation intravenous cephalosporin with broad spectrum effectiveness against numerous gram-negative bacteria, such as E.coli, and P. aeruginosa, as well as gram-positive bacteria including staphylococci and streptococci (Kessler, Bies et al. 1985). In contrast to other cephalosporins like ceftriaxone, cefoperazone, cefotaxime, and ceftazidime that are having resistance to some bacteria like S. aureus and β-lactamases, Cefepime drug is highly stable against β-lactamases (Kessler, Bies et al. 1985, Fung-Tomc, Dougherty et al. 1989).

1.3. Epidemiology of bacterial infection

Advanced medical practices are in danger due to the emergence of Gram-negative bacteria (GNB) that are multi-, extensively-, and globally drug-resistant (Magiorakos, Srinivasan et al. 2012). It is frequently more difficult to treat infections due to the current lack of antibiotic alternatives. Four of the six most prevalent infections linked to antimicrobial resistance (AMR)-related mortality (almost a million fatalities were linked to AMR in 2019) are GNB (Murray, Ikuta et al. 2022). Beta-lactamases, or enzymes that inactivate many beta-lactam antibiotics, can be produced by a variety of enterobacteria (including Klebsiella pneumoniae, Escherichia coli), as well as lactose non-fermenting GNB (including Pseudomonas aeruginosa). In 2010 in Thailand, Lim and colleagues evaluated the global impact of multidrug resistance in six bacterial pathogens (Lim, Takahashi et al. 2016), and in 2014, Temkin and colleagues analyzed the prevalence of Escherichia coli and Klebsiella pneumoniae resistance to third generation cephalosporins and carbapenems in 193 countries (Temkin, Fallach et al. 2018).

According to the Reviews on Antimicrobial Resistance, six pathogens—HIV, tuberculosis, malaria, S aureus, E coli, and K pneumoniae—were responsible for 700 000 fatalities in 2014. CJL Murray and his colleagues calculated the number of deaths caused by resistance to four of those pathogens—tuberculosis, S aureus, E coli, and K pneumoniae—at 670,000 in 2019 (Murray, Ikuta et al. 2022).

1.4. Antibiotic diversity

Here are a few examples of the wide variety of antibiotics and their molecular targets: Vancomycin, cephalosporins, and penicillin (including methicillin) all work by attacking the bacterial cell wall. Sulfa drugs_ growth factor analogues, Quinolones_ effect DNA gyrase, Tetracyclines_ effects the bacterial ribosome. Rifampin_ targets nucleic acid metabolism. All target processes specific to the bacteria without harming the host.

1.5. Frequent consumptions of antibiotics in Pakistan

After China and India, Pakistan is the country that consumes the most antibiotics that is disappointing news. Without visiting a doctor, people often use antibiotics excessively. Researchers estimate that Pakistan has 50,000 unregistered pharmacies and more than 60,000 quack medical practitioners who like to prescribe such medications. The unnecessary use of antibiotics in Pakistan is caused by a variety of circumstances.

Self-medication and polypharmacy are the main causes, followed by factors like a higher percentage of lack of education, wasteful consumption, and the sale of antibiotics without a prescription. Pakistan is a developing nation with a lot of diseases and few resources. As a result, some opt for antibiotic treatment instead of a doctor's prescription. People with even less resources can utilize antibiotics since they are widely available at low prices. Recently, 550 samples of drug medications were gathered by a drug inspector and sent for analysis. Well over nine brands of antibiotics were discovered to be fakes and imposters. The World Health Organization advises only taking antibiotics on a doctor's or physician's prescription. Since consuming too many medications decreases their effectiveness and promotes resistance. Additionally, in an analysis, Researchers kept track of AMU (antimicrobial use) in 30 flocks from a commercial broiler farm in Punjab, Pakistan's most populated province, from 2013 to 2017.

Antimicrobial dosage was determined using both the used daily dose (UDD) and milligrams per population unit of the final flock weight (mg/fPU). The amount of active component used annually on farms was 250.84 mg per kilograms of final flock weight. Except for China, every country in the world uses more antimicrobials per kilograms of chickens more than this consumption level. Their research indicates that up to 568 tons of antimicrobials may be consumed annually in Pakistan's broiler industry. The first baseline investigation of the usage of antibiotics in animals in Pakistan has revealed a startlingly high consumption prediction. Such findings demand immediate action to decrease the usage of antibiotics in Pakistan and other nations with similar agricultural practices (Mohsin, Van Boeckel et al. 2019).

1.6. Origin of antibiotic resistance

When a medication or drug agents starts to fail to effectively reduce bacterial growth, antibiotic resistance occurs. Bacteria become immune to antibiotic activity and can continue to grow. Whenever bacteria reproduce even when antibiotics are present, they are referred to as resistant bacteria. If the bacteria are more resistant or less vulnerable, a higher concentration of same medicine is required. Immediately following the introduction of novel antibacterial chemicals, antimicrobial resistance was discovered. Frequently administered antibacterial chemicals are comparable to and located close to agricultural antibiotics, which can promote medication resistance. One possible explanation for the transmission of antibiotic-resistant bacteria between

animal and human populations is through the food chain. Food, water, or parents who may have microbial resistance to a particular antibiotic are the main sources of antibiotics for livestock.

The utilization of antibiotics as growth promoters leads to an increase in antibiotic resistance in cattle feed. Research of the rural areas in Barcelona has revealed that one-fourth of the neonates were found to have a fecal carrier of Quinolone-resistant Escherichia coli, with poultry or swine as a potential source. Quinolones have been administered to these kids (Mubeen, Ansar et al. 2021).
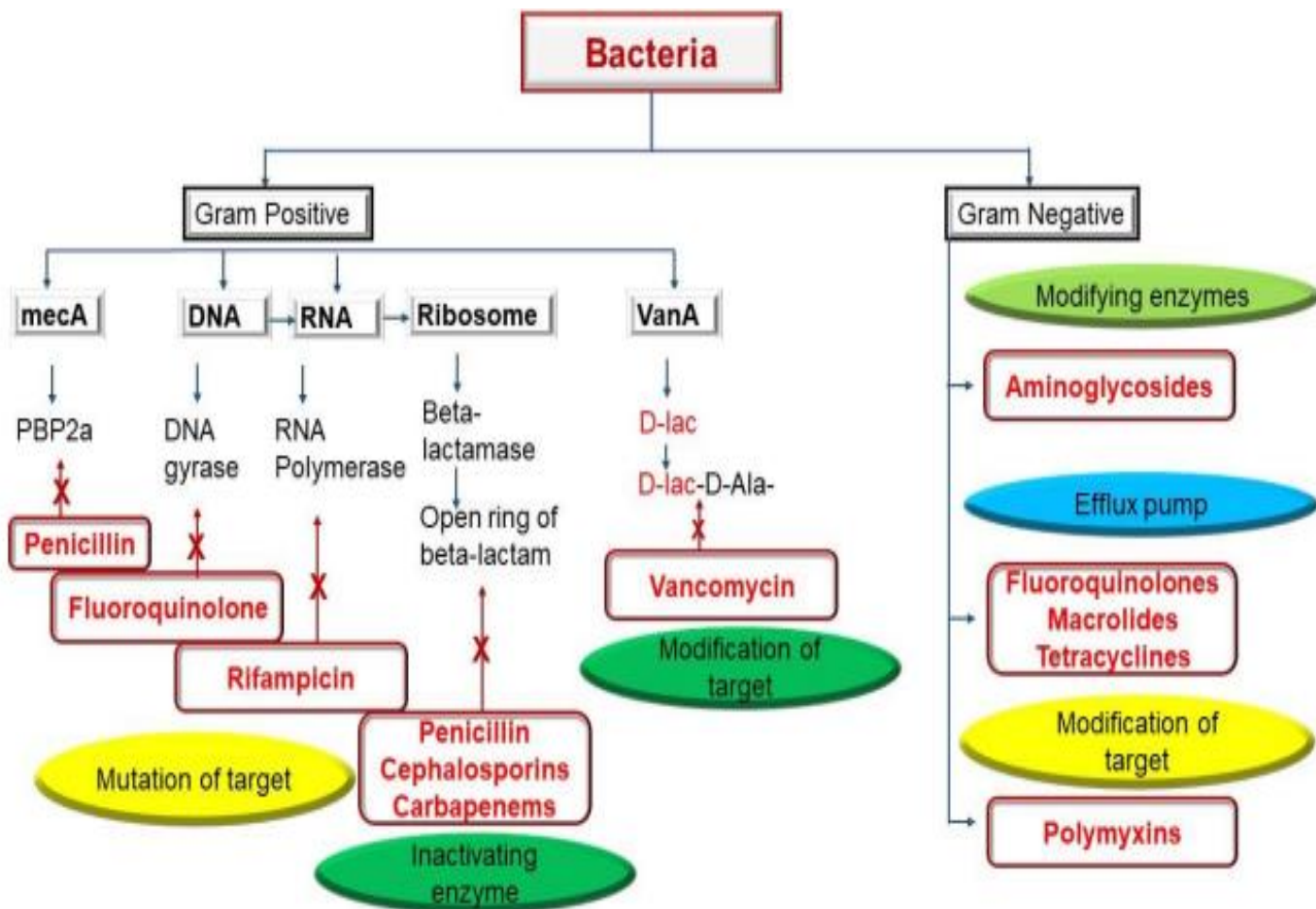
Figure 1. Reveals that there are different mechanisms through which bacteria develop resistance to antibiotics involving: Drug binding site alteration, increased production of altered target sites, substitution of target sites, ejection or decreased permeability, enzyme inactivation and modifications.

1.7. Availability of antibiotics

Additionally, experts in infectious diseases and microbiology have advised against overusing antibiotics. In certain instances, medical practitioners restrict the use of the most recent drug

because they fear it may encourage resistance and instead continue to provide current antibiotics that have previously demonstrated comparable efficacy. Therefore, in the fight against severe diseases, new medications are frequently used as the "final line" of defensive medicine. This strategy restricts the use of contemporary medications while lowering investor returns. Many pharmaceutical businesses worry that the millions of dollars needed to research new antibiotics won't yield enough profit (Mubeen, Ansar et al. 2021).

1.8. Methicillin Resistance Staphylococcus aureus (MRSA)

The Gram-positive cocci bacteria Staphylococcus aureus (S. aureus) is frequently detected on human skin and mucous membranes. This bacterium has the potential to spread up to 30% of the world's population. Although being a natural component of the human microbiome, it is a bacterium that can cause a variety of illnesses, from minor skin conditions like boils and rashes to serious conditions like chronic bacteremia, sepsis, and pneumonia.

Toxicity or diseases caused by this bacterium is related to a wide range of virulence factors, including adhesins, enzyme and toxin synthesis, synthesis of biofilm, and immune system evasion mechanisms. This invasive organism is most recognized for its terrifying reputation due to its antibiotic-resistant phenotype, which is in addition to the known virulence characteristics.

1.9. Emergence of Nanotechnology in the era of Antibiotic Resistance

Antibacterial medications enter cells through enhanced diffusion or active transport mechanisms. By gaining resistance to antimicrobial drugs, which results in the generation of resistant variants, some germs gain the capacity to adapt, persist, and advance, such as methicillin-resistant Staphylococcus aureus (MRSA) and vancomycin-resistant bacterium Enterococci. Some pathogens can now be said to follow the multidrug resistance rule. These microbes may acquire MDR due to their inherent virulence, capacity to cause a wide range of fatal illnesses, and adaptability to different environmental factors.

The consequence of the widespread proliferation of these adaptable microorganisms involves prolonged infection and increased costs. Drug inactivation, a decrease in binding sites, and decreased permeability can all happen occasionally (Eko, Forshey et al. 2015). Certain ways to combat this antibiotic resistance, including limiting the usage of antimicrobial drugs, steering clear of ineffective antimicrobials, creating new medications, and harnessing therapeutic

nanotechnology for drug manufacture (Laxminarayan, Duse et al. 2013, Akhtar, Swamy et al. 2015, Tuli 2019).

The nanoparticles have been regarded as novel strategies due to their unique physicochemical properties such as toughness, long-lasting efficiency, and flexibility. The improvement in the field of nanotechnology presents the fabrication of various nanosized inorganic/organic molecules with potential application in the fields of medicine, therapeutics, and diagnostics sectors with a significant effect on improving human well-being (Wong, Bhatia et al. 2013, Thabit, Crandon et al. 2015, Tuli 2019). The creation of these nanoparticles as antimicrobial substances demonstrates that a different strategy can be used to address the issue of antimicrobial resistance since nanoparticles use entirely different processes than conventional antibiotics (Akhtar, Swamy et al. 2015).

1.10. Critical role of Nanotechnology as an Improved Drug Delivery System

One of the most advanced developments of the twenty-first century is known as nanotechnology (Reese 2013). Unique physico-chemical characteristics of nanoscale materials have been employed in several manufacturing and industrial sectors and are anticipated to revolutionize the domains of biotechnology, medicine, and pharmaceuticals. Nanotechnology may offer remedies to many of the unresolved problems in modern medicine relating to the prevention, diagnosis, and treatment of diseases, providing advantages for healthcare professionals, specific patients, and society broadly (Leso, Fontana et al. 2019).

Rapid development for the creation of improved drug delivery systems is necessary for improving dosage forms. Due to their delivery method, programmed target-specificity, cellular uptake, clearance, toxicity, metabolism, pharmacokinetics, excretion, greater half-life in terms of repeated drug administration, and enhanced patient health, modified drug delivery systems have been thought to transport drugs that are in greater demand (Tibbitt, Dahlman et al. 2016).

Successful drug delivery systems are made to use internal or external stimuli to boost the medication's effectiveness in the body, and the characteristics of the nanocarriers are altered in accordance with the physicochemical characteristics of the pharmaceuticals (Tong, Pan et al. 2020). To promote patient compliance, medications need to have a biocompatible encapsulation and a highly effective, regulated release (Tong, Pan et al. 2020). The fundamental structure needed for the creation of new and improved drug delivery systems is taken into consideration

because of the quick growth in research in the field of polymer science (George, Shah et al. 2019).

Drug delivery systems have mostly used non-biodegradable polymeric nanoparticles including polymethylmethacrylate, polyacrylamide, and polystyrene; nevertheless, non-biodegradable polymers have been found to be extremely toxic and to have negative health effects. As a result, the scientific community is debating the use of biocompatible polymers for in vivo and in vitro illness detection and therapy due to their vast attributes as well as development (Ramkumar, Pugazhendhi et al. 2017, George, Shah et al. 2019, Hassan and Zhang 2019).

Biodegradable polymers degrade both enzymatically and non-enzymatically, producing a harmless by-product that is biocompatible. Targeted drug delivery applications place a noticeable focus on the chemistry of newly developed molecules in the case of biodegradable polymers. The adverse consequences of a certain medicine are lessened using biocompatible polymers. Biodegradable biomaterials have good permeability, good therapeutic capabilities, and no ongoing inflammatory effect (Prajapati, Jain et al. 2019).

CHAPTER 2. LITERATURE REVIEW

2.1. Cephalosporins

Cephalosporins, formerly known as Cephalosporium, was identified in 1945 and has been investigated for a long time. Since all antibiotics come from natural sources, natural cephalosporins originate from a fungus called Acremonium. Since this class of antibiotics has been studied for many generations and has a history of developing resistance, they have been divided into five different generations as more and more research has been done on them (Mehta and Sharma 2016).

Cephalosporins, also known as beta lactam antibiotics, are used to treat various diseases caused by both gram-positive and gram-negative bacteria. Meningitis, resistant bacteria, skin infections, and several other infectious ailments can all be treated with the five generations of cephalosporins (Bui and Preuss 2023). The first generations of cephalosporin function against gram-positive bacteria, while further generations are highly active against gram-negative bacteria.

2.2. 4th generation of cephalosporin

Among the 4th generation cephalosporins, which also include cefpirome, cefoselis (FK-037), and combinations of the latter drugs with catechol-containing cephems (i.e., cefetecol), only cefepime has been utilized as a treatment for a substantial amount of surgically acquired infections (Giamarellou 1993, Giamarellou 1996). A fourth-generation cephalosporin antibiotic known as cefepime hydrochloride has been classified as a beta-lactam antibiotic. Cefepime possesses an extra quaternary ammonium group, which improves its ability to pierce gram-negative bacteria's outer membrane.

This medication has the bactericidal activity against both Gram-positive i.e., staphylococcus aureus and Gram-negative i.e., E-coli, Klebsiella pneumonia bacteria. It is useful for the management of bacterial infections like pneumonia, complicated and uncomplicated urinary tract infections, skin and soft tissue infections, complicated intra-abdominal infections (in combination with metronidazole) (Chapman and Perry 2003, Rivera, Narayanan et al. 2016).

Figure 2. Structure of cefepime HCL

2.2.1. Mechanism of action

Cefepime's mode of action is like those of other beta-lactam antibiotics. By covalently binding with the enzymes required for the last stage of transpeptidation during the synthesis of peptidoglycan walls, cefepime inhibits the formation of bacterial cell walls. This binding causes defects in the cell wall leading the organism to perish from autolysis (self-destruction). Cefepime is more resistant to beta-lactamases as opposed to third generation cephalosporins. and has enhanced gram-negative coverage because of certain processes. Among such processes one is reduced affinity of Penicillin-binding enzymes for cefepime. Another one is that it has a different chemical structure from earlier generations due to the replacement of a side chain, which increases its effectiveness against staphylococcal species (Kessler 2001, Chapman and Perry 2003).

2.2.2. Dosage

Cefepime ought to be taken intravenously (IV) or intramuscularly (IM) because the gastrointestinal tract cannot effectively absorb it. The preferred method of administration is IV, and 1 to 2 g are frequently administered every 8 to 12 hours, based on the infection being tackled. Injections are typically given over the course of 30 minutes. Research findings that compared longer infusions of 4 hours to the typical 30-minute rate found lower overall mortality and shorter stays in intensive care units (ICUs). Some studies, however, were unable to replicate

these results. The feasibility of treating febrile neutropenia with extended infusion rates has been examined (Bauer, West et al. 2013, Wrenn, Cluck et al. 2018, Zhu and Zhou 2018).

2.2.3. Adverse effects

Both adolescents and pediatric patients often handle cefepime effectively. The most typical side effects in adults include redness and diarrhea. Fever, diarrhea, and rash are the most frequent side effects in children. Numerous additional, less frequent negative consequences are stated in accordance with the system impacted, including neurological symptoms like headache, fever, and neurotoxicity, gastrointestinal, hepatic damage, colitis, including pseudomembranous colitis, oral candidiasis, nausea, vomiting, and abdominal pain, renal damage, vaginitis, and genitourinary.

The serious, even fatal adverse effect of neurotoxicity demands special attention. Alterations in mental state, encephalopathy, seizures, myoclonus, hallucinations, coma, and symptoms that resemble a stroke are all possible signs. Typically, four days after taking cefepime, symptoms appear. Renal failure (creatinine less than or equal to 60 mL/min), ageing adults, critically ill ICU patients, strokes, Alzheimer's disease, brain cancer, a history of seizures, and a weakened blood-brain barrier (BBB) are risk factors. According to the proposed procedure, Cefepime has the ability to cross blood brain barrier and suppress gamma-aminobutyric acid receptors (Deshayes, Coquerel et al. 2017, Payne, Gagnon et al. 2017).

With renal impairment, it's crucial to monitor and modify dosage; nonetheless, there have been cases of neurotoxicity in patients with healthy kidneys as well (Appa, Jain et al. 2017, Huwyler, Lenggenhager et al. 2017, Isitan, Ferree et al. 2017).

2.3. Antibacterial resistance towards cephalosporins

Penicillin binding proteins (PBP, peptidoglycan transpeptidase) help bacteria to construct a stronger cell wall by cross-linking peptidoglycan units. The broad class of bactericidal antibiotics known as cephalosporins was first created from the fungus Cephalosporium species. Their beta-lactam rings allow them to operate as intended. The beta-lactam rings attach to the penicillin-binding protein, preventing it from performing its intended function. Bacteria that cannot produce cell walls will die. A bacterial species, Staphylococcus aureus, that is responsible for causing different infections including skin and skin structure infections, can change the structure of the penicillin-binding proteins to develop resistance. S. aureus possesses a gene that codes for

a modified penicillin-binding protein to avoid the beta-lactam rings of the cephalosporins from deactivating the protein. The development of such a resistance strategy is caused by a bacteria termed methicillin resistant Staphylococcus aureus (MRSA) (Bui and Preuss 2023).

Only the fifth generation "Ceftaroline fosamil" of the five cephalosporin generations, as was previously stated, offers defense against MRSA. Additionally, another strategy used by bacteria to resist penicillin is the creation of the enzyme beta-lactamase, which disassembles the beta-lactam ring and prevents it from attaching to proteins that bind penicillin, such as peptidoglycan transpeptidase. Researchers established an alternate method of attack to get around this problem, combining beta-lactamase inhibitors with cephalosporins to increase their spectrum of activity, as in the examples of ceftazidime/avibactam and ceftolozane/tazobactam (Bui and Preuss 2023).

Moreover, an enormous number of bacterial organisms are showing resistance towards beta-lactam antibiotics, called extended spectrum beta-lactamase (ESBL) generating pathogens. Even though Cefepime is ineffective against the majority of ESBL infections, it is sensitive to a subtype of ESBLs known as Amp-C producers. Despite the possibility that some organisms are cefepime sensitive, a comprehensive assessment of the minimum inhibitory concentration (MIC) and the dose schedule is necessary before therapy to ensure adequate treatment (Nguyen, Shier et al. 2014, Walker, Lee et al. 2018, Patel, Lusk et al. 2019).

There are two main ways that S. aureus can withstand beta-lactams: first, by using -**lactamases** to render the antibiotic inactive, and second, and more dangerously, by using a **low affinity PBP2a**

NH₃⁺

Extracellular

BlaR1/MecR1

Intracellular

Zn⁺²

COO⁻

Active BlaI

blaR1 | blaI | blaZ

Inactive Protease

In absence of β-lactams, the **Transcriptional repressors** BlaI and MecI exist as dimers and block the transcription of *blaz* and *mecA*

mecR1 | mecI | mecA

Active MecI

Transcription of **mecA** and **blaZ** blocked by MecI and BlaI

BlaR1 and **MecR1** are acylated by the antibiotics

Beta-lactamase

NH₃⁺

PBP2a

Cefepime HCL

Activation of a zinc **protease**

Cleaves **BlaI** and **MecI**

Extracellular

BlaR1/MecR1

Intracellular

Zn⁺²

COO⁻

Transcription of *blaZ* and *mecA*

blaR1 | blaI | blaZ

Protease cleaves MecI and BlaI

Production of **β-lactamase** (encoded by *blaZ*) and **PBP2a** (encoded by *mecA*)

mecR1 | mecI | mecA

Transcription of **mecA** and **blaZ** are now allowed

Figure 3. Molecular mechanism of antibiotic resistance by S. aureus

2.4. Alternative approach to combat antibacterial drug resistance

The lack of new, efficient antibiotics is the primary reason for the rise in resistance among bacteria. This has inspired projects around the world to create more potent antibacterial substances to tackle the issue of antibiotic resistance (Hassan, Kamal et al. 2012, Rai, Deshmukh et al. 2012, Rudramurthy, Swamy et al. 2016). Scientists are quite anxious, and they are looking into every avenue they can to find a solution to the antimicrobial resistance issue. Treatment of

bacterial infections with nanoparticles is a more critical and potential approach. Innovative developments in nanotechnology, particularly the creation of methods and tools for creating NPs with specific properties, are anticipated to lead to the creation of novel nano-antimicrobials.

Nanoparticles have unique physical, chemical, structural, mechanical, electrical, and optical features making them highly efficient and attractive antibacterial agents, in addition to having a high surface-to-volume ratio (Whitesides 2005, Hajipour, Fromm et al. 2012, Jeevanandam, Barhoum et al. 2018). Additionally, they have essential qualities that draw researchers and developers to this field of study and development, including their capacity to interact with the bacterial cell barrier, suppression of bacterial protein and DNA production, and regulation of bacterial metabolic activities (Wang, Hu et al. 2017).

It has been notified that the advancement in nanotechnology to treat infectious diseases, particularly skin diseases, includes two major areas: the first encompasses the use of materials having antimicrobial capacities at the nanoscale; the second requires the incorporation of recognized medications into nano-vehicles for better release and improved effectiveness (Cunha-Azevedo, Silva et al. 2011, Domínguez-Delgado, Rodríguez-Cruz et al. 2011, Kumar, Agarwal et al. 2011).
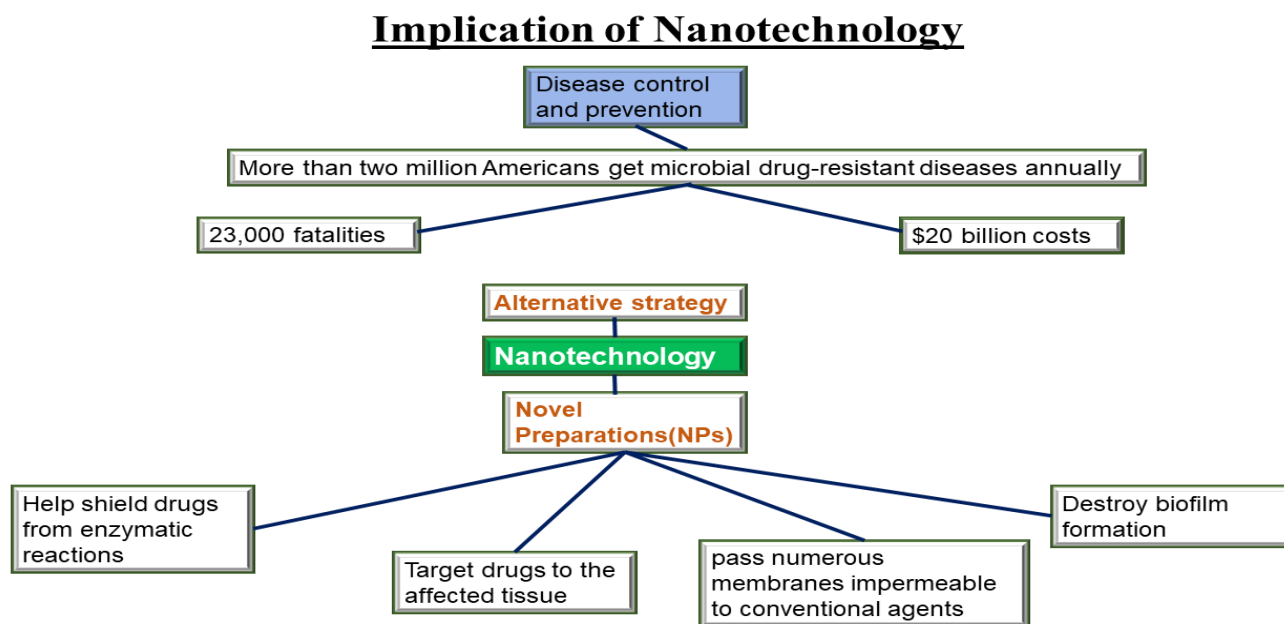
Figure 4. Manifesting the application of nanotechnology

2.5. Polymeric nanoparticles as novel drug delivery system

Based on their shape and physicochemical properties, novel drug delivery systems are categorized as Carbon-based nanoparticles, polymeric nanoparticles, metal nanoparticles, ceramic nanoparticles, semiconductor nanoparticles, lipid-based nanoparticles, and others. Out of all of these, polymeric nanoparticles are one that has received the most attention by researchers due to both its benefits over other areas and the rapid development of polymer science and nanotechnology.
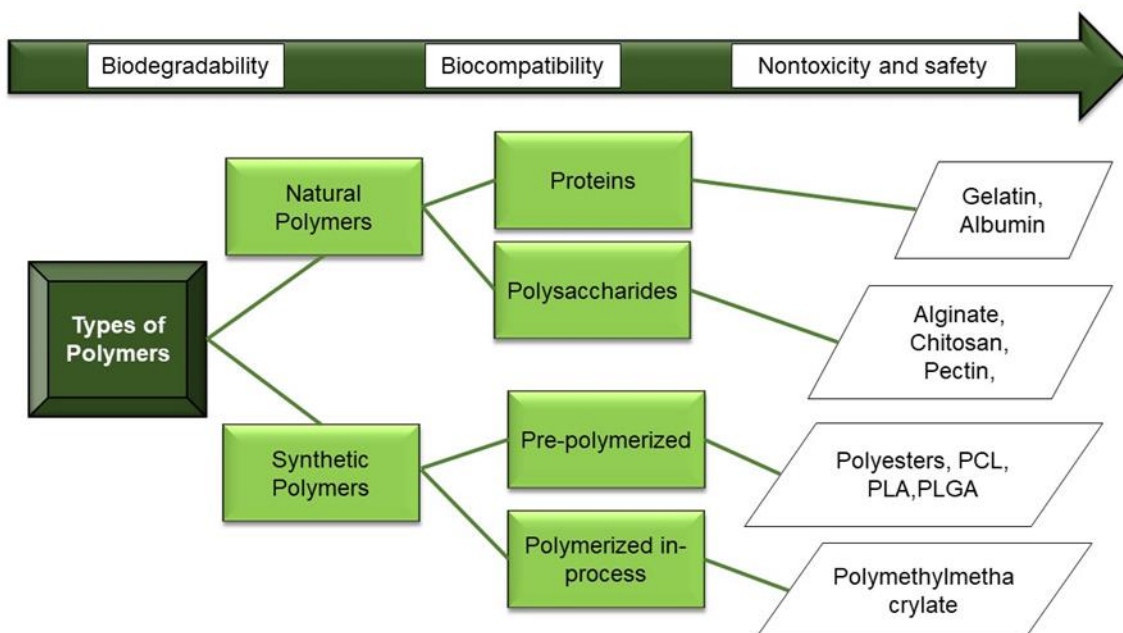
Figure 5. Demonstrates important features of the polymeric nanoparticles and classification of polymers with examples.

Polymeric nanoparticles have several benefits, including an accessible preparation process, controllable size distribution, good drug retention and protection, etc. Biodegradability and biocompatibility are two important features that permit such polymeric nanoparticles to be preferable for drug delivery (Sur, Rathore et al. 2019). Peter Paul Speiser created the first nanoparticles for targeted medicine administration in the late 1960s. In 1994, polymer nanoparticles came into existence. Numerous researchers began creating nanoparticles with various polymers and began observing the benefits and drawbacks of doing so. Because of the biodegradability of polymer and safety, biodegradable polymer nanoparticles have drawn attention. Biodegradable polymer nanoparticles have several advantages over non-biodegradable

polymer nanoparticles, including the fact that they are non-immunogenic, non-allergenic, less poisonous, and do not need to be removed from the body because the polymer breaks down there (Ahmed, Mora-Huertas et al. 2013, Wen, Hsu et al. 2019).

Table 1. Ceftriaxone loaded polymeric nanoparticles against MRSA

Drug loaded polymeric Nanoparticles	Method	Size	Zeta Potential	Entrapment Efficiency	Bacterial strains	In-vitro analysis
Ceftriaxone loaded polymeric nanoparticle (**Mushtaq, Khan et al. 2017**)	Ionic Gelation Method	220nm	-36.88mV	35-40%	*E.coli, S. aureus*	Zone of inhibition: 23mm for MRSA strains, 25mm for E. coli
Ceftriaxone loaded chitosan nanoparticle (**Duceac, Calin et al. 2020**)	Ionic Gelation Method	250nm	38.5mV		*E.coli, S. aureus*	Enhancing anti-bacterial activity by suppressing gram (+Ve), gram (-Ve) microorganism proliferation

2.6. Chitosan as powerful natural nanocarrier against bacterial skin infections

The most suitable material for use in the creation of a topical therapy for microbial infection of the skin would be a nanomaterial with strong natural antibacterial properties and the ability to function as a nano-vehicle. Chitin, the primary building block of the exoskeleton of crustaceans, is the source of the natural polysaccharide biopolymer known as chitosan. Depending on the degree of deacetylation, chitosan may include several C2 amino groups with pKa values of 6.5, which can become protonated in mildly acidic conditions.

This polycationic composition of chitosan confers its antibacterial properties, which favor interaction with negatively charged microbial cell walls and cytoplasmic membranes. Reduced osmotic strength, membrane rupture, and subsequent intracellular element release are the results of those events (Sanpui, Murugadoss et al. 2008, Banerjee, Mallick et al. 2010). Additionally, by interacting with bacterial DNA, chitosan may reach the nuclei of bacteria and prevent the generation of mRNA and proteins (Qi, Xu et al. 2004, Ma, Zhou et al. 2008, Blecher, Nasir et al. 2011). The surface-to-volume ratio of chitosan increases when it is scaled down to the nanoscale, leading to higher surface charge density, a stronger affinity for bacteria and fungi, and enhanced antibacterial activity (Qi, Xu et al. 2004). A notable increase in the solubility in aqueous acidic conditions can be achieved because chitosan has a lower degree of N-acetyl groups than chitin (Pillai, Paul et al. 2009).

Since chitosan has fewer N-acetyl groups, more primary amines can be protonated under acidic circumstances, increasing its solubility to somehow. Chitin's limited solubility in both aqueous and organic solvents limit the uses for which it can be used. By enhancing the solubility properties of chitosan, the practical application of this natural polymer in various industries—including the food, cosmetic, textile, and medicine sectors, to name a few—is significantly enhanced (Pillai, Paul et al. 2009).

2.6.1. Previous analysis on chitosan coated antibacterial cephalosporins

Several findings have demonstrated that chitosan nanoparticles (CHN-NPs) have enhanced antibacterial efficacy against S. aureus and E. coli because of their potential to carry medicines (Qi, Xu et al. 2004, Kong, Chen et al. 2010). Additionally, Chitosan-dependent drug carriers may improve the therapeutic effectiveness of the antibiotic by extending its release and reducing its side effects to reduce ceftriaxone resistance (Lee, Kim et al. 2005, Azhdarzadeh, Lotfipour et al. 2012, Shanmugarathinam and Puratchikody 2014, Duceac, Marcu et al. 2019, Duceac, Mitrea et al. 2019, Ichim, Duceac et al. 2019, Luca, Eva et al. 2020). Balya, H et al., created cefixime nanoparticles that showed great encapsulation effectiveness with sustained drug release for up to 28 h and were made via the fruit mucilage and chitosan of the Azadirachta indica. In comparison to pure cefixime, the produced compound demonstrated greater in vitro antibacterial effectiveness. The results of the in vivo oral acute toxicity assessment thoroughly supported the conclusion that the produced formulation was safe for biomedical applications. Moreover, continuous treatment of rats with a cefixime preparation showed much greater weight loss in the

organs as opposed to rats treated only once with free cefixime, indicating an increase in antimicrobial action. These findings imply that the gradual clearance of the cefixime preparation may be responsible for the antimicrobial activity impact. Such useful outcomes have proved that the prepared formulation is an ideal delivery system with enhanced oral bioavailability and greater treatment effectiveness compared to the free cefixime drug, Thereby, acquiring appreciating patient compliance as opposed to the commercial preparation of cefixime (Balya, Radhakrishnan et al. 2021).

To add more, the drug Ceftazidime is frequently used to treat ocular infections, especially those brought on by P. aeruginosa. However, since ceftazidime rapidly degrades in aqueous solutions, there are currently no commercially accessible eye drops that contain the drug Ceftazidime. Furthermore, the barriers that surround the eye prevent eyedrops from entering the ocular globe. To tackle such issues, Ceftazidime was enclosed in nanoparticles made of chitosan/TPP (tripolyphosphate)-Hyaluronic Acid. The size, zeta potential, and ceftazidime encapsulation effectiveness of the nanoparticles were studied to improve a nanoparticulate system for a prospective eye drop formulation.

Furthermore, investigations on in vitro drug release and penetration were conducted, and the findings point to a sustained drug release from the nanoparticles. The results of the interaction of nanoparticles with mucin show their mucoadhesive and capacity to engage with the ocular surface, extending the duration of medication residence in the eye. The produced NPs successfully underwent stability and microbiological investigations (Silva 2016). Finally, in vitro tests supported earlier published data in which the NP formulation demonstrated 100% cell survival by demonstrating that NPs were not harmful to the examined cell lines (de la Fuente, Raviña et al. 2010).

2.7. Different strategies for the preparation of chitosan nanoparticles

Ohya and co-workers first discovered chitosan nanoparticles in 1994. They delivered an anticancer drug 5-flourouracil by formulating chitosan nanoparticles using emulsification and cross-linkage protocols (Grenha 2012). Afterwards, a variety of techniques were used to create Chitosan NPs. There are currently five alternatives. These are polyelectrolyte complex, ionic gelation, microemulsion, covalent cross-linking, and reverse micellar technique (Tiyaboonchai 2013). Ionic gelation and polyelectrolyte complex are among these, and these are the most often

employed techniques. These techniques are straightforward and don't involve the use of organic solvents or significant shear forces (Sailaja, Amareshwar et al. 2011).

2.7.1. Ionic gelation method

By aggregating chitosan or its derivatives with biomolecules that have opposite charges to one another or in the presence of an ionic cross-linking agent, ionic cross-linking is accomplished using this approach. The most often utilized cross-linking agent is tripolyphosphate. This technique is also known as the ionic-gelation method because it results in the development of gels because of ionic linkage (Avadi, Sadeghi et al. 2010). Chitosan NPs encapsulating Estradiol (E2) are made by ionic gelation method using trisodium polyphosphate as a cross linker, and they have a zeta potential of +25.4 mV and size of average 269.3nm (Nagpal, Singh et al. 2010).

2.7.2. Covalent Cross linking

The functional cross-linking agent and chitosan, or its derivatives, establish covalent bonds in this approach. Polyethylene glycol, glutaraldehyde, and monofunctional agents are examples of frequently utilized substances (Prabaharan and Mano 2004).

2.7.3. Reverse Micellar Method

In this process, an aqueous chitosan solution is combined with an organic solvent which contains a surfactant. Agitation occurs simultaneously. Water is added to the mixture to keep it in an optically transparent microemulsion phase. The amount of water is increased to create NPs that are larger. Using this method, chitosan nanoparticles (NPs) were made to encapsulate the doxorubicin-dextran conjugate.

2.7.4. Nanoprecipitation/Coacervation

This method is based on the physicochemical properties of chitosan, notably on its precipitate formation and the insoluble nature in alkaline pH conditions. Coacervate droplets are produced by pouring the chitosan solution into the alkali solution using a compressed air nozzle. Following filtering or centrifugation, the particles are then cleaned by being washed repeatedly in both hot and cold water. In this way, chitosan-DNA nanoparticles are produced (Agnihotri, Mallikarjuna et al. 2004).

2.7.5. Polyelectrolyte Complex

As a result of charge neutralization between the cationic charged polymer and DNA, which results in a reduction in hydrophilic characteristics, the cationic charged polymer and plasmid DNA self-assemble into polyelectrolyte complexes. The CHN NPs can spontaneously develop

when DNA solution is introduced to chitosan that has been dissolved in acetic acid while being mechanically stirred at room temperature (Erbacher, Zou et al. 1998).

2.8. Topical drug delivery through gels

In case of topical drug administration, medications are directly applied to the skin at the targeted site, enhancing the concentration of the drug in the localized area and minimizing the drug concentration in the systemic circulation (Elsayed, Abdallah et al. 2007). Numerous studies have shown that topical delivery vehicles, like ointments (creams, gels, and pastes), have more benefits than drawbacks (Yadav, Yadav et al. 2021). More precisely, cutaneous administration of medications promotes patient compliance, drug's bioavailability, and quick distribution of medication to the targeted area. Anyhow, some of the drawbacks like poor penetration or skin irritation have been mitigated by the introduction of biocompatible materials and penetration enhancers (Yuan, Pan et al. 2022). Nanogels can be prepared using a variety of synthetic and natural polysaccharide-based polymers, including chitosan (CS), pullulan, hyaluronic acid, dextran, and carbopol 940 (Aderibigbe and Naki 2018). Carbopol 940, also known as Carbomer 940, is a synthetic polymer with a high molecular weight derived from acrylic acid monomers. Carbopol 940 consists of 56% to 68% carboxylic (–COOH) groups (Mohanambal 2010). In a neutral pH aqueous solution, Carbopol 940 acts as an anionic polymer, wherein many side chains lose protons and attain a negative charge. This characteristic enables Carbopol 940 polyelectrolytes to absorb and retain water, causing them to swell significantly, reaching several times their original volume (Gutowski 2010).

The primary objective of this research is to formulate and evaluate carbopol gel loaded with cefepime nanoparticles as a topical delivery system for combating bacterial skin infections. Cefepime nanoparticles were created through an ionic gelation method utilizing, chitosan as a positively charged polymer and sodium alginate as a negatively charged polymer, cause cross-linking among them. A model was designed with design expert software to optimize these nanoparticles. The resulting optimized nano-formulation was introduced into a solution containing carbopol 940 to create a carbopol nanogel. Comprehensive characterization studies were conducted for both the nanoparticles and the nanogel. Furthermore, the applications were explored by examining cumulative drug release and conducting antibacterial assays.

CHAPTER 3. MATERIALS AND METHODS

3.1. Chemicals and materials

- Cefepime HCL (commercially available) was kindly gifted from Quaid-i-Azam University Islamabad, Pakistan that was purchased from Shaigan Pharmaceuticals Pvt. Ltd. Islamabad, Pakistan.

- Chitosan (CHN) with a moderate molecular weight and a degree of deacetylation ranging from 75-85% (Sigma-Aldrich, Germany) was used to encapsulate cefepime HCL drug.

- Tween 80(Daejung Chemical and Materials CO-LTD, Korea) was used as a surfactant.

- Sodium Alginate (Daejung Chemical and Materials CO-LTD, Korea) with a purity of 90% used as a cross-linking agent.

- Other analytical chemicals like NaOH, ethanol, glacial acetic acid (99.5% purity) (Merk, Germany) were used as received.

- Phosphate buffer solution, Mueller-Hinton II Agar (MHA) and Nutrient agar (Biolab Diagnostic laboratory, Budapest, Hungary) were used for bacterial growth.

- Deionized water was used for making solutions and dilutions and for washing purpose throughout the experiment.

- Carbopol-940 polymer (ordered from Sigma Aldrich) was utilized as a thickening agent for gel preparation.

- Tri-ethanolamine was used as a gelling agent for making gel.

3.1.2. Bacterial strains

Clinical isolates of *Staphylococcus aureus* (ATCC 6538) and *Escherichia coli* (ATCC 8739), *K. pneumonia* (ATCC 43816) bacterial strains for antibacterial assays were obtained from the Atta-ur-Rehman School of Applied Biosciences (ASAB, NUST).

3.1.3. Apparatus used for Experimentation

(a) 50 ml beakers for making solutions and for nanoparticles synthesis purpose.

(b) 10 ml vials.

(c) 10 ml and 5ml pipettes for liquids measurement.

(d) Magnetic stirrer bars for stirring purpose.

(e) Glass slides for microscopic observations.

(f) Dropper for solution addition on glass slides.

(g) Double ended spatula for transferring dry chemicals from one apparatus to another.

(h) 0.22µm and 0.45µm syringe filters for filtration of nanoparticles before performing zeta sizer.

(i) 3ml, 5ml, and 10 ml syringes for injection of one solution into another.

3.1.4 Equipment for experimental purpose

(a) Hotplate (wise stir) used for magnetic stirring purposes and maintaining fixed temperature.

(b) UV spectrophotometer (BMS-UV-2800).

(c) Vacuum oven (FISTREEN OVA031) for drying purposes.

(d) Sonicator (Cole Parmer) for proper mixing.

(e) Centrifuge machine (Siemensstr, 25, HERMLE Labortechnik GmbH) for obtaining pellet and supernatant independently.

(f) PH meter (JENWAY) was used to find out the pH of formulations.

(g) Electronic weighing balance (SHIMADZU) used for the measurement of dry chemicals and materials.

(h) FTIR machine (Perkin Elmer) was used for FTIR study.

(i) Analytical Scanning Electron Microscope (JSM-6490A) and ion sputtering device (Automatic gold meter) (JFC-1500) was used to conduct SEM analysis of samples.

3.2. Methodology
3.2.1. Preparation of blank chitosan/alginate nanoparticles

The ionic gelation method was employed to produce chitosan– sodium alginate nanoparticles (Abdelghany, Alkhawaldeh et al. 2017). For the preparation of blank chitosan/alginate (CHN-Alg) nanoparticles, CHN solution (0.2%) was prepared in 10 ml of aq. acetic acid (1% volume/volume) in a glass vial with overnight stirring at 850 RPM to achieve complete dissolution. Add 15 mg of the surfactant (Twee-80) to the chitosan homogenized solution and agitate with a magnetic stirrer for approximately 40 min to completely dissolve it. The pH of the chitosan solution was maintained to 5 using 0.5M NaOH. As a cross-linker, 10 ml of sodium alginate solution (0.05%) was prepared, and the pH was adjusted to 5 using 0.5M HCL. After PH maintenance of both solutions, inject the sodium alginate solution dropwise through a syringe while continuously stirring at 1200 rpm on a hotplate set at 30°C. The solution was stirred for 2 h to ensure complete interaction between the two oppositely charged CHN and ALG molecules until a clear, miscible solution was obtained.

3.2.2. Preparation of cefepime-loaded chitosan/alginate nanoparticles

To prepare drug loaded CHN/Alg nanoparticles using the ionic gelation technique as shown in fig (6), the same procedure was followed unless a constant amount of drug was used. For drug-loaded chitosan nanoparticles, make a solution of 3 mg of drug in deionized water. This drug solution was then injected into the chitosan solution (0.2%). Further steps were followed as discussed above for the preparation of blank nanoparticles. The resultant drug-loaded chitosan nanoparticle suspension was then centrifuged for approximately 45 min in three cycles at 14,000 rpm using a high-speed centrifuge (HERMLE Labortechnik gmbh Germany). After discarding the resulting supernatant, the pellets were lyophilized (freeze dried) for future use.
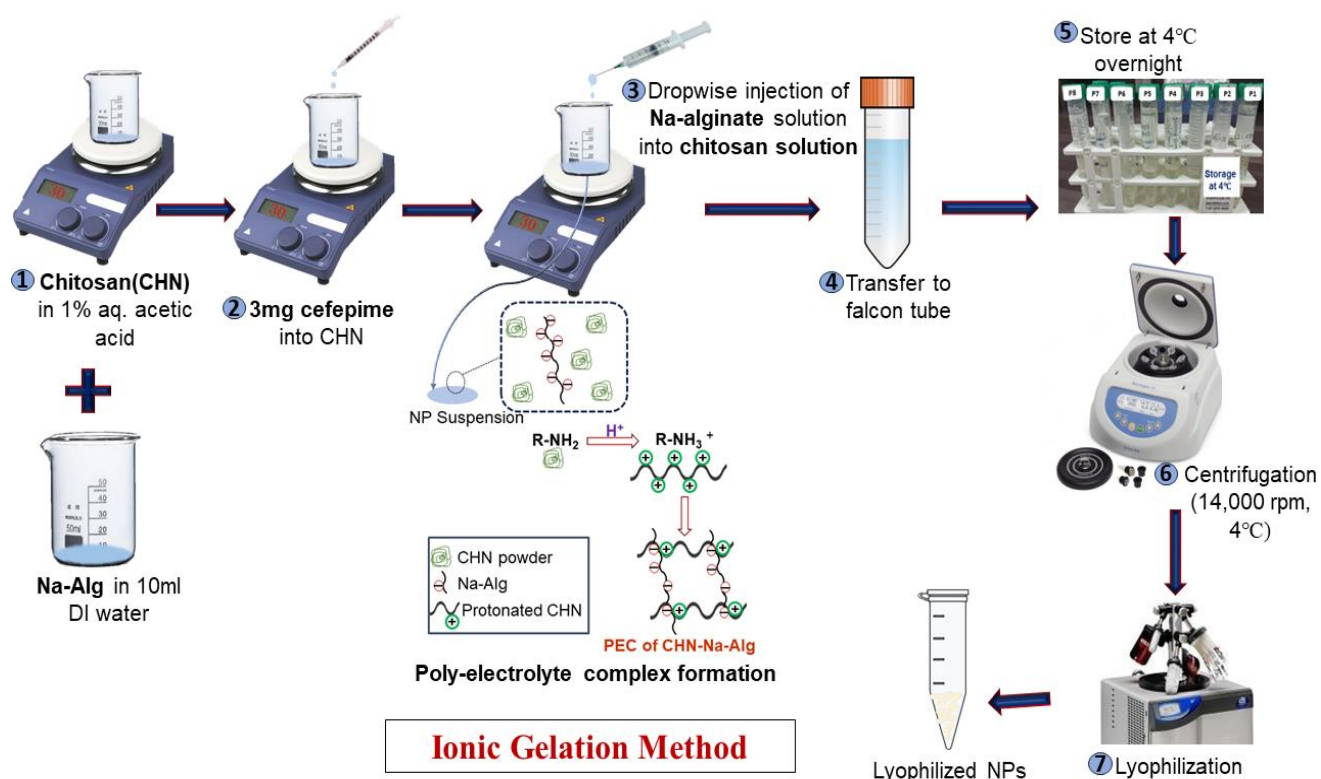
Figure 6. Formation of drug-loaded chitosan/alginate nanoparticles by ionic gelation method

3.2.3. Optimization of cefepime-loaded chitosan nanoparticles

State-ease design expert software (version: 13.0.5.0) was employed to optimize the antifouling cefepime-loaded nanoparticles (CEF-NPs). The objective was to achieve the intended outcomes by adjusting the polymer concentration, stirring time, and injection rate. The variables to be studied were surfactant(tween-80), stirring time, and injection rate with predetermined ranges. The range for surfactant concentration was 5-15mg, stirring speed was 60-120, and injection rate

was 30–40. A randomized factorial design was used, and the software designed eight different runs using 2 level factorial design. An experimental design plan created using design expert software is shown in Table 2.

To assess each run of the software provided, three dependent variables, namely, the size of the cefepime-loaded nanoparticulate suspension, zeta potential, and encapsulation efficiency (E.E), were used. The key goal was to obtain a lower size, higher zeta potential value, and maximum encapsulation efficiency. Statistical studies were conducted using the 3FI model based on the significance of the responses indicated by the F-value, R^2 -value, and accuracy of the results. ANOVA was used to evaluate the data, and when each response was demonstrated to be significant (p-value <0.05), graphs were created to illustrate how independent factors affected the various responses. The link between single and multiple variables was examined using one factor and a three-dimensional surface graph.

3.2.4. Cefepime nanoparticle- loaded carbopol gel formation

The gel of the optimized formulation was designed to deliver chitosan nanoparticles optimized for cefepime loading and to manage cefepime release over an extended period. Hydrogel was prepared using 1% Carbopol 940. Carbopol 940 and deionized water were added to a 50-ml beaker and stirred for 4 h until a smooth and viscous solution was obtained. To prepare the drug loaded Carbopol gel, the optimized formulation was injected into the already prepared Carbopol viscous solution under constant stirring. Once all solutions were homogenized, 2 to 3 drops of triethanolamine were added to the solution to achieve neutralization and cross-linking (ÇAĞLAR, GÜVEN et al.). This cross-linking causes the mixture of carbopol–drug–nanoparticle formulation to form a gel-like consistency.
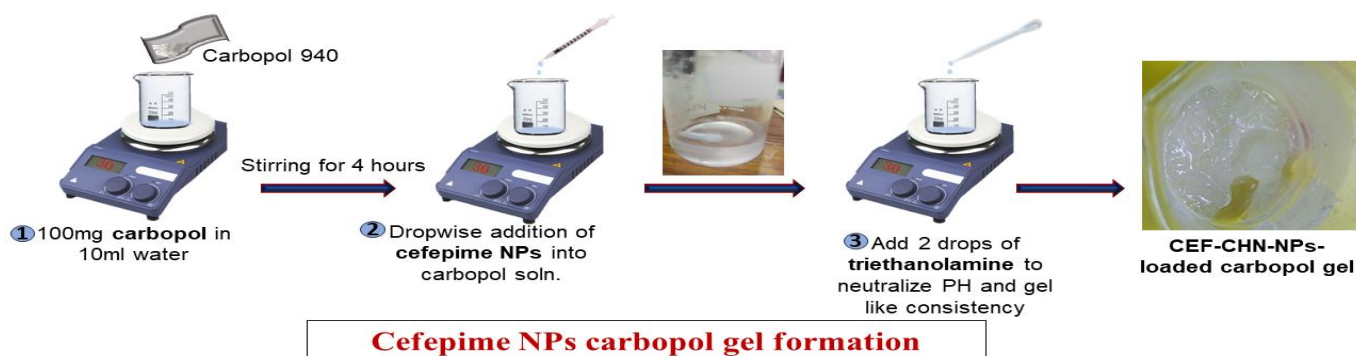
Figure 7. CEF-CHN-NPs loaded gel preparation.

3.3. Different characterization techniques for evaluating cefepime- loaded chitosan nanoparticles

3.3.1. Stability studies by physical appearance

After the formulations were prepared, they were stored in a refrigerator at 4℃. The developed formulations were physically observed for 90 days. The formulations were analyzed for precipitate formation and phase separation.

3.3.2. Dynamic Light Scattering (DLS) Zeta sizer

A Zeta sizer (Malvern Nano ZS-90, UK) containing software version 6.34 and operating on the principle of dynamic light scattering by a He– Ne laser was used to assess all eight-formulation analyses provided by a state-ease design expert for particle size and PDI. The zeta potentials of all formulations were also analyzed using an electrophoretic light scattering protocol. The results of each sample were obtained in triplicate at scattering angle 90°. The sample was prepared in such a way that about 10µl of formulation was diluted in 990µl for both zeta potential and size. The outcomes are presented as the average particle size determined by analyzing three distinct batches, all of which were examined thrice.

3.3.3. Scanning electron microscopy (SEM)

Using scanning electron microscopy (SEM), the morphology of the nanoparticles (NPs) was characterized. To prepare a sample for SEM analysis, the emulsion was centrifuged and then washed to remove any layer or impurities from the particles. Then, one drop of that emulsion was diluted with deionized water, followed by the addition of one drop of the diluted emulsion to the glass slide and spreading that drop on the slide to make a thin layer. It was then oven dried at 29° for overnight. To characterize the sample using the SEM machine, the specimens were coated with gold using an ion sputtering device. The SEM machine then produces digital images of various parts of the sample at various magnifications using a voltage of 20 kV. The images were then analyzed to identify the shapes and sizes of the optimized blank and cefepime-loaded particles.

3.3.4. Fourier transform infrared spectroscopy (FTIR)

FTIR analysis was performed using an FTIR machine (Perkin Elmer spectrum 100 spectrometer). FTIR studies were performed to examine how the various elements of the optimized preparation interacted with one another by comparing their functional groups. For this purpose, KBr was mixed with nanoparticles either in suspension or powder form, and pellets

were created using a hydraulic press and then examined. The frequency range for scanning the specimens was 4000 to 400 cm^{-1}.

3.3.5. X-ray diffraction analysis

The crystalline nature of the substances required to make the nanoparticles involving cefepime HCl, chitosan, sodium alginate, blank, and drug-loaded nanoparticles—was examined by XRD (Theta, STOE German) evaluation. XRD patterns of all ingredients were created at a wavelength of 2.54Å and an intensity range of 10°–90°.

3.3.6. UV Spectrophotometer

UV analysis was carried out in a solution of drug mixed with DI water in which the DI water was run as control. Four milliliter of solution was placed in a special UV quartz cuvette, and then the UV machine was run on the sample using UV software on the computer to determine the absorbance spectra of the drug in DI water. The UV spectrum was run within the range of 200-700 nm to find λ_{max} of the cefepime drug.

3.3.7. Entrapment Efficiency

One of the main metrics for inspecting the effectiveness of the nanoencapsulation method is the entrapment efficiency (EE). For this purpose, the formulations were centrifuged for 45 min at 14000 rpm. The pellet was discarded or stored for further use, and the supernatant was scrutinized to determine the free drug at λ_{max} (291nm). The captured drug was obtained by subtracting the free cefepime drug from the total cefepime used in the preparation (Fan, Wu et al. 2008).

$$\text{Entrapment Efficiency (\%)} = \frac{\text{Total cefepime} - \text{Free cefepime in supernatent}}{\text{Total cefepime}} \times 100 \qquad (1)$$

3.4. Characterization of the cefepime nanoparticle- loaded Carbopol gel

3.4.1. Physical appearance and pH testing

The gel dosage form containing cefepime-loaded chitosan nanoparticles was visually evaluated for color, homogeneity, clarity, and matter texture (Al-Hamadani and Al-Edresi 2022). Its physical attributes were also compared with those of a commercially available drug in gel form. Using an electronic PH meter (JENWAY, 3510 PH meter), the pH of the carbopol gel-loaded nanoparticles was determined. For this purpose, we weighed 0.5 g of gel, dissolved it in 10 mL of deionized water in a beaker, and left it for 1 h. To determine the pH, an electrode from a pH-meter was brought into contact with the gel solution and left there for 1–2 min to reach

equilibrium. Subsequently, measurements were recorded three times and the average values were calculated (El-Enin, Khalifa et al. 2019).

3.4.2. Gel spreadability

Gel spreadability was measured by filling a 2 cm (θ) rectangle drawn on a glass slide with 0.5 g of carbopol gel. A second glass slide was positioned on top of the first glass slide, and a weight of 100 g was applied to the upper glass slide (Ahad, Al-Saleh et al. 2017). After spreading (A2), the diameter of the gel was recorded at intervals of 1 and 2 min. Spreadability in percentage was calculated using the following formula:

$$\text{Spreadability \%} = (A2)/\theta \times 100 \qquad (2)$$

3.4.3. Viscosity testing

The viscosities of the carbopol gel loaded with CEF-CHN-NPs and the carbopol gel containing the marketed medication were measured using a spindle-64 and a viscometer (DV-I Prime Brookfield Viscometer) for comparison (Kazim, Tariq et al. 2021). For each sample, the viscosity values in centipoise (cp) were determined by altering the stirring speed (RPM) (Al-Hamadani and Al-Edresi 2022).

3.4.4. Drug Content

Drug content analysis was performed to assess the homogeneous distribution of cefepime in the carbopol gel. 0.1 g of gel was dissolved in 10mL of deionized water. The mixture was vortexed for five min for complete dissolution. The solution absorbance was determined at 291 nm using a UV spectrophotometer (Kazim, Tariq et al. 2021).

3.5. In vitro drug release study at two different PH

Utilizing the dialysis bag diffusion approach as described in previous studies (Binesh, Farhadian et al. 2021, Imam, Gilani et al. 2023), the in vitro release of cefepime from the optimized CEF-CHN-NPs and from the CEF-CHN-NP- loaded carbopol gel was assessed in comparison with free cefepime. Phosphate buffer solutions (PBS) with pH 5.5 and pH 7.4 were prepared for the release study. The dialysis membrane bags with a molecular cut-off of 12 kDa were filled with a suspension of CEF-CHN-NPs with 3 mg of drug, pure drug solution for comparison, and CEF-CHN-NPs loaded gel, and then immersed in 50 mL PBS solution at pH 5.5 and 7.4. Subsequently, the system containing 50 ml of PBS acting as a receiver compartment along with a dialysis bag (donor compartment) was put in the incubator shaker, which was adjusted to 100

rpm and 37 °C. At predefined time intervals (0.5, 1.0, 2.0, 4.0, 8.0, 12.0, 24 hours), we extracted 2 mL samples and replenished the containers with an equal volume of fresh media to ensure consistent solubility conditions. The concentration of cefepime in the released media was quantified using a UV spectrophotometer at 291 nm. The same procedure was carried out independently for CEF-CHN-NPs containing 3 mg CEF, CEF-CHN-NPs loaded gel, and 3mg of free CEF and was conducted three times. The cumulative percentage of drug release was plotted over time. To analyze the data, linear regression equations for both pH values of PBS were applied, and the order of drug release from various formulations was documented.

Several kinetic models that are applied to a medication's in vitro release profile offer insight into the release mechanism of the drug. The present study employed multiple release models, including Korsmeyer Peppas, Higuchi, and Hixon Crowell first-order and zero-order models, to analyze the cefepime release data from NPs, CEF-NP- loaded gel, and cefepime control solution.

3.6. In vitro antibacterial activity of formulations using the agar well diffusion method

The antibacterial efficacy of optimized blank and cefepime-loaded Nano formulations as well as gel was assessed against Gram-positive and Gram-negative microorganisms, including Staphylococcus *aureus* (ATCC 6538) and *Escherichia coli* (ATCC 8739). A protocol of agar well diffusion assay was employed to determine the antibacterial activities of the optimized formulations and the gel (Balouiri, Sadiki et al. 2016). First, freshly made nutrient gar was poured onto a plate labeled with E. coli and S. aureus, followed by picking one colony of both strains and streaking, which were then incubated at 37 °C for an entire night. Using a sterilized inoculum loop, bacterial colonies were picked from freshly prepared cultivated media and placed in a 1 mL saline solution that had been previously autoclaved. For the sake of a uniform distribution of the bacterial inoculum in the saline solution, it was vortexed for five minutes. The optical densities were then adjusted using 0.5 McFarland standards (Gonelimali, Lin et al. 2018). 100 mm Petri dishes were filled with 150 mL of the MHA solution while a burner was located beneath a laminar flow hood. To screen for contamination, the solidified agar plates were stored overnight at 37 °C in an incubator. Each Petri dish's center was filled with 60 microliters of microbial culture using a micropipette, and then swabbed with cotton buds that had been sterilized. Three 9-mm wells were made on the ager plate using sterile blue tips: one for the sample (suspension or gel) labeled as sus or gel, one for the pure drug-loaded solution as well as gel labeled as positive control, and one blank formulation marked as negative control. 50µl of

each sample is inserted through 100 µl of pipette and incubated for 24 h at 37°C. After 24 h of incubation, uniform bacterial growth was observed with zones of different diameters, which were measured in mm using a graduated scale.

CHAPTER 4. RESULTS

4.1. Formulation and optimization of cefepime-loaded CHN-Na Alg-NPs

Various concentrations of independent variables, including Surfactant (tween 80), stirring speed, and injection rate along with their corresponding responses in terms of nanoparticle size, zeta potential and encapsulation efficiency, are presented in Table 2. Run number 7 was chosen by the software with the objective of achieving the smallest nanoparticle size and maximum encapsulation efficiency.

Table 2. Experimental design of regular two-level factorial design

	Independent Variables			Dependent Variables		
Code	Chitosan mg	Stirring time min	Injection rate ml/min	Size nm	Zeta Potential mv	Encapsulation Efficiency %
P1	5	120	0.25	670	15.3	65.33
P2	5	60	0.25	700	9.48	62.67
P3	5	60	0.33	721	9.15	62
P4	15	120	0.33	294	17	82.5
P5	5	120	0.33	684	14.4	64
P6	15	60	0.25	407	16	73
P7	**15**	**120**	**0.25**	**230.5**	**18**	**80**
P8	15	60	0.33	591	16	73.33

4.1.1. Performance of the design expert software to statistically assess experimental outcomes

The outcomes of the study setup demonstrated that the surfactant concentration, stirring time, and injection rate had an impact on the particle size (PS), zeta potential (ZP), and percentage of EE (entrapment efficiency). The 3FI model was selected based on the largest R^2 value (Table 3).

Table 3. Depicts the recommended model and regression R2 values indicating the fitness of model for all responses.

Responses	*Model*	*R^2 value*	*Adjusted R^2*	*Predicted R^2*	*Adequate precision*
Particle Size	3FI	0.9866	0.9532	0.7862	14.0397
Zeta Potential	-	0.9957	0.9850	0.9315	24.8061
Entrapment Efficiency	-	0.9971	0.9900	0.9544	28.9751

Table 2 shows that the predicted R^2 values are in agreement with the adjusted R^2 values, i.e., the difference is less than 0.2. Adequate precision measures the signal-to-noise ratio. A ratio greater than 4 is desirable. All these values of adequate precision signify an adequate signal. Additionally, the R-squared values of all responses (i.e., 0.9866, 0.9957, and 0.9971) demonstrated the model's outstanding match to the real data.

4.1.2. Variance Evaluation (ANOVA)

To evaluate the level of significance of the outputs and quantitative impacts associated with the suitable models, a statistical approach of ANOVA was used (Iftikhar, Iqbal et al. 2020). The effects of variables A (surfactant concentration), B (stirring time), and C (Injection rate) on outcomes are outlined in Tables 3. A= PS, B = ZP, and C= EE, are the responses. At 95% confidence level, the model seemed significant (p <0.05). The value and sign of the quantitative effect indicate the likelihood and degree of importance of the factors determining the response, respectively. The regression equation's negative (-Ve) value shows an antagonistic relationship between the factor and response, whereas a positive value expresses a synergistic relationship.

Table 4. Manifests F-value and P-value showing significancy and appropriateness of chosen variables.

Parameters	Effect	F-value	P-value
R1 (Particle size)			
A	-313.25	107.68	0.0092
B	-135.125	20.05	0.0464
C	70.625	5.48	0.1441
AB	-101.625	11.34	0.0780
AC	53.125	3.10	0.2204
Average		29.53	0.0331<0.05
R2(Zeta potential)			
A	4.6675	263.09	0.0038
B	3.5175	149.42	0.0066
C	-0.5575	3.75	0.1923
AB	-2.0175	49.15	0.0197
AC	0.0575	0.0399	0.8601
Average		93.09	0.0107<0.05
Entrapment Efficiency (%)			
A	13.7075	584.38	0.0017
B	5.2075	84.34	0.0116
C	0.2075	0.1339	0.7495
AB	2.8775	25.75	0.0367
AC	1.2075	4.53	0.1676

Average		139.83	0.0071<0.05

The F-values of all responses (i.e., R1, R2, and R3) demonstrated that the model was significant. The highest F-value of the variable surfactant (584.38) proved the term's significant impact on entrapment efficiency. In addition, a smaller p-value is desired because it indicates that the related variables are appropriate. The parameters with a 95% confidence level ($p < 0.05$) specifically showed a significant impact on responses. Consequently, the surfactant concentration (Tween 80) was the most critical element in this study, as indicated by a P-value of 0.0017 (Guo, Ren et al. 2009).

4.1.3. Statistical analysis of responses by one factor and 3D surface plot

Responses of all eight formulations were also statistically analyzed using 3D surface plots and single factor graphical representations that were displayed one by one.

4.1.3.1. Particle size

The particle size of the optimized cefepime-loaded chitosan nanoparticles (**P7**) obtained by DLS was 230.5 with a PDI value of 0.214, representing the monodispersity of the formulation, as shown in Fig (8). Particles greater than 300 nm were also obtained, but the maximum intensity between 200 and 300nm indicated that more particles were acquired in this region.
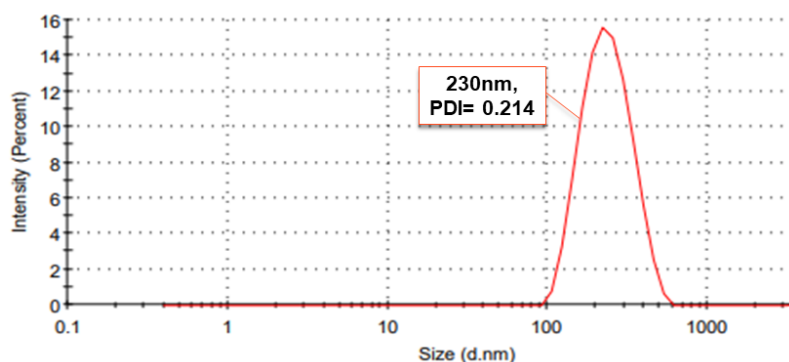
Figure 8. Average hydrodynamic size and PDI value

The particle size of nanoparticles is influenced by several variables. These variables include surfactant (Tween 80) content, pH, chitosan, stirring time, and injection rate. Several compositions were created by changing each variable individually to determine the effects of these factors. Each preparation's particle size, zeta potential, and EE were assessed separately. Table 1. shows results of particle size, zeta potential, and EE for various preparations. The

Tween-80 content was increased to reduce particle size because surfactants reduce interfacial tension and improve the solubility and stability of nanoparticles, which reduces particle size (Zargartalebi, Kharrat et al. 2015). Another study revealed equivalent patterns (Gul, Ahmed et al. 2018). For the eight preparations, various variables were combined to produce particle sizes ranging from 230.5 to 721nm. Figures 9(a) and (b) show how variable change affects particle size.

(a)

(b)
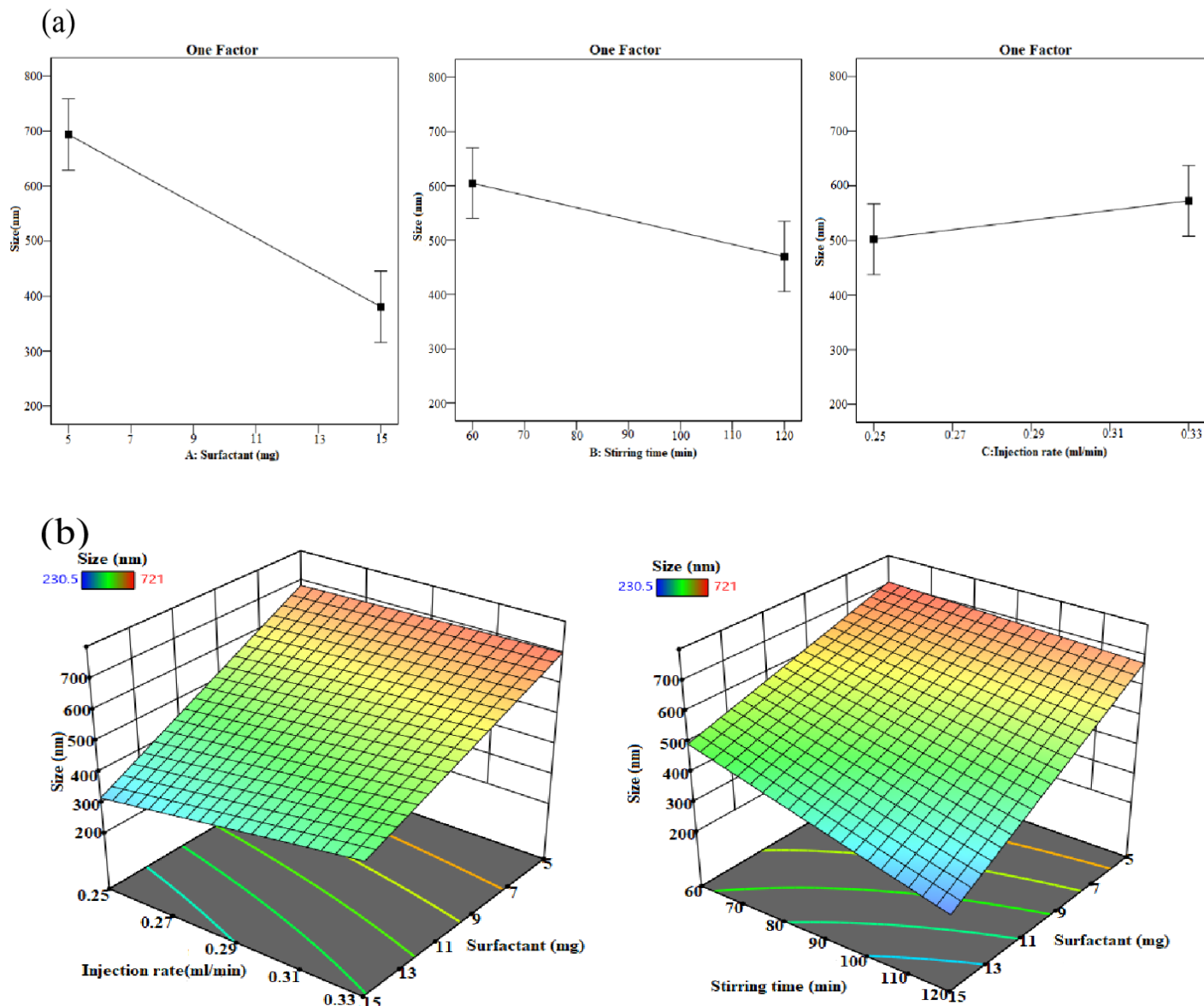
Figure 9. (a) Demonstrates how several factors determine nanoparticle size. Particle size is inversely correlated with stirring time and surfactant concentration. The particle size is somewhat influenced by

injection rate. (b) Three-dimensional graphs demonstrating the simultaneous effects of two parameters on particle size.

4.1.3.2. Zeta Potential

An essential attribute that demonstrates the stability of nanoparticle composition is the zeta potential of NPs. The zeta potential value of formulations greater than 11 represents the stability of the nanoparticles. The zeta values of all eight preparations varied from 9.15 to 18 mV. Positive ZP values indicate that only some amino groups are neutralized during NP formation (Berthold, Cremer et al. 1996).
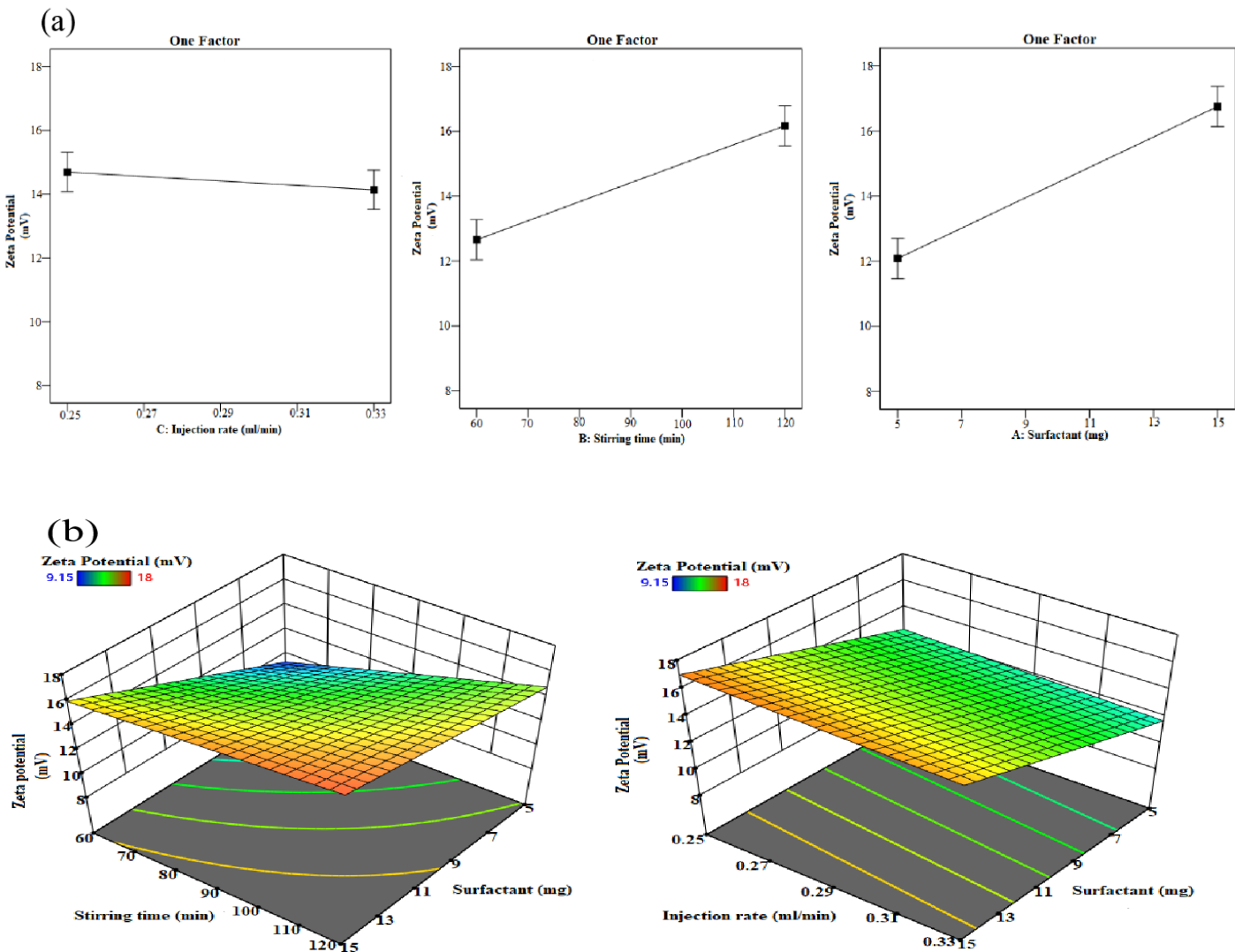
Figure 10. (a) 1-D plot and (b)3-D plot reveals the direct relationship between the zeta potential of a nanosuspension, surfactant content, and stirring time. but there is some influence of the injection rate on the zeta value.

The zeta potential of optimized cefepime-loaded chitosan nanoparticles (**P7**) obtained by DLS is 18mV representing high stability of the formulation as shown in fig 11.
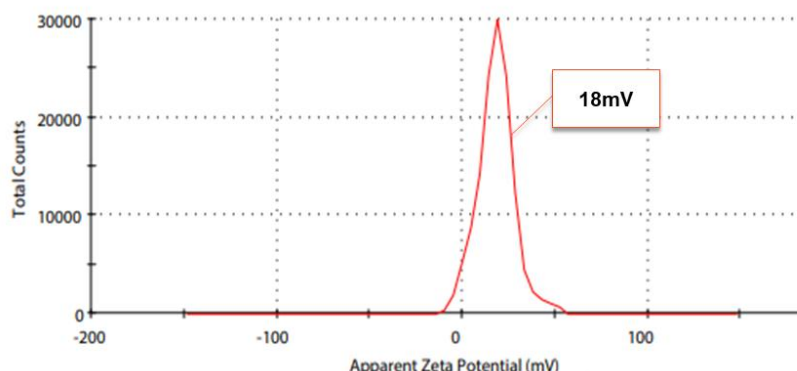
Figure 11. Zeta result of cefepime loaded-chitosan nanoparticles

4.1.3.3. Entrapment Efficiency

For all eight formulations, the percentage of encapsulation efficiency varied from 62 to 82.5. The acquisition of the highest R^2 value (0.9971) of EE for 3FI model represented the most significant variable and the fitness of model. Factors such as surfactant concentration was significantly affecting the entrapment of cefepime in chitosan nanoparticles. In comparison to chitosan microparticles, small particles in the nanoscale range retain a large surface area causing the particles to encapsulate more drug (Iftikhar, Iqbal et al. 2020). Encapsulation efficiency of all eight NPs preparations is shown in one factor plot (fig 11(a)) and 3D response surface plot (fig 12(b))

(a)
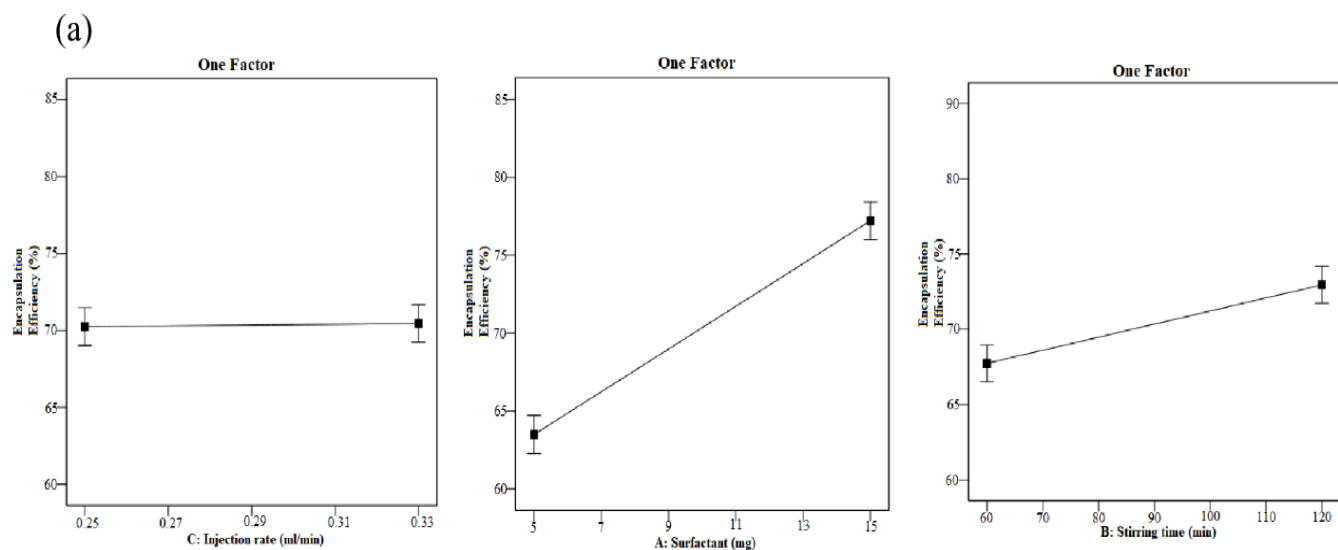
(b)
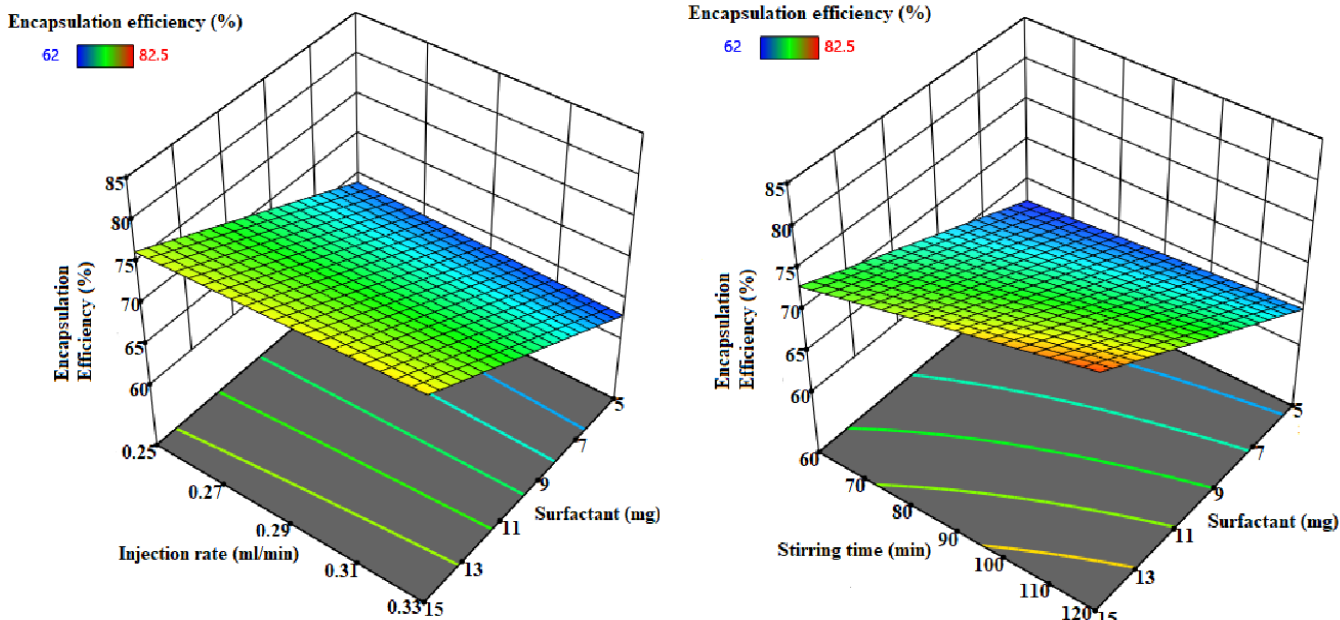
Figure 12. (a) 1-D plot and (b)3-D plot Illustrates that, compared to stirring duration and injection rate, the surfactant concentration has a greater impact on entrapment efficiency. Surfactant concentration and entrapment effectiveness are directly correlated.

The entrapment efficiency of the optimized formulation is 80%. This increment in the encapsulation capacity of particle is because of its small size, large surface area and most importantly the moderate surfactant concentration i.e., 15mg. This entrapment efficiency is obtained by plotting a graph of the absorbance of different aliquots of stock solution of drug. The regression equation was obtained by this graph giving the absorbance of unknown sample.

4.2. Evaluation of the morphology of chitosan nanoparticles by scanning electron microscopy (SEM)

SEM was used to examine and describe the distinct exterior morphology of the optimized drug-loaded and blank preparations. The figures display SEM images at 2,500, 5,000, and 10,000x magnifications at a voltage of 20kv as shown in fig (14). The nanoparticles were observed to be somehow irregular but mostly spherical expressing nano capsules with a mean diameter of blank formulation of 156.71±12.75nm, as shown in fig. 14(b) and for drug loaded as 221.75±56nm as shown in fig. 14(d). Approximately similar size ranges were observed in previous studies (Talib, Ahmed et al. 2021).
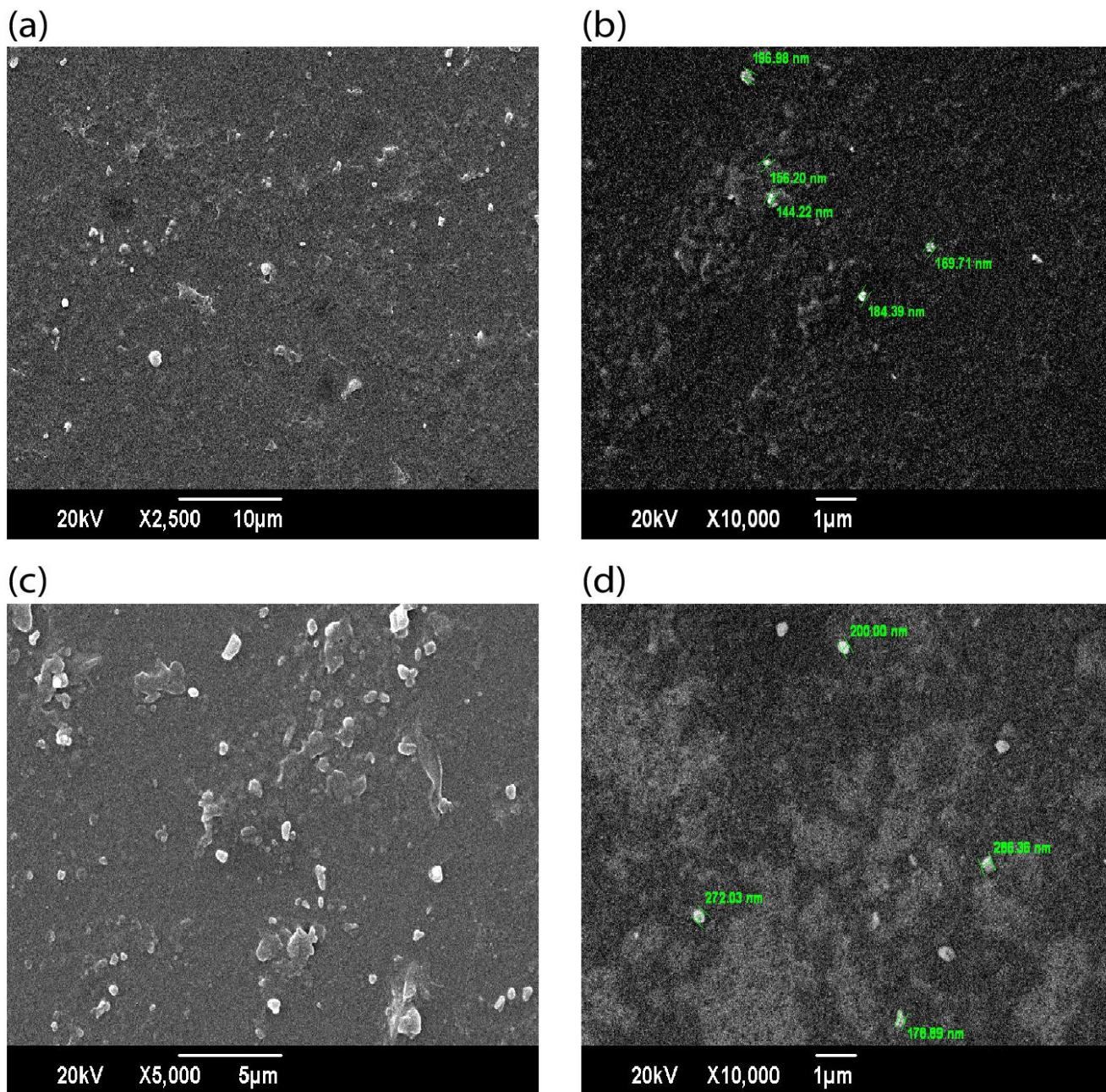
Figure 14. SEM results of blank (a and b) and drug-loaded (c and d) preparations at different magnifications.

4.3. Evaluation of the modifications of characteristic peaks using FTIR

The FTIR spectra of pure chitosan, sodium alginate, cefepime HCL, blank and drug laded chitosan-alginate nanoparticles are presented in fig (15). Multiple peaks are found in distinct frequency ranges in FT-IR spectra, and each frequency level represents a separate functional group or vibrational band (Coates 2000). The characteristic peaks in the IR spectra of CHN are

presented at wavenumbers 3425cm-1, 2879 cm-1, 1660 cm-1, 1596 cm-1, 1387 cm-1, 1079 cm-1 depicting broad band of hydroxy(O-H) and amino(N-H) group, peak originated by -OH stretching, C-O stretching vibration of amide-I band, bending vibrations of N-H amide-II band, N-H stretching of amide-III band, and secondary hydroxyl group (C-O stretch), respectively. Moreover, the specific characteristic peaks observed for Na Alg are given in wavenumbers as 3420cm-1, 2930 cm-1, 1620 cm-1, 1413 cm-1, 1095 cm-1, and 1025 cm-1 expressing wide N– H and O-H stretch, C-H stretch, asymmetric stretching of carboxylate salt group, symmetric stretching of -COO-, C-O-C bending vibration, C-O-C stretching(representing saccharide structure of sodium alginate), respectively (Li, Dai et al. 2008, Ahmad, Greish et al. 2022). Considering cefepime HCl peaks for N– H and O-H stretch, beta-lactam C=O stretching, amide C=O stretch and primary alcohol (C-O stretch) were observed at 3370cm-1, 1777cm-1, 1648cm-1, and 1043cm-1. Functional groups present at these characteristic peaks of pure polymers and the drug show that there is compatibility among them (Ferdous, Sultan et al. 2015). As opposed to the FTIR spectra of pure materials, the characteristic peaks of blank chitosan nanoparticles are 3465cm-1, 1417cm-1 revealing N– H and O-H stretch, and carboxylate group(-COO-) respectively. Here, we can observe the absence of the NH2 bending peak at 1596cm-1 because of the interaction of Na-Alg with CHN forming nanoparticles. Furthermore, in the spectra of the synthesized cefepime-loaded chitosan-alginate nanoparticles, peaks appeared at 1626cm-1 and 1416cm-1 showing shifting of asymmetrical stretch of -COO- as well as of symmetric stretch of -COO- respectively and at 1097cm-1 represents C-N amino group and the CH2 bend for drug. In addition, there is a shifting of stretching vibrations of O-H and N-H bonds at characteristic peak 3429cm-1 of drug loaded nanoparticles.
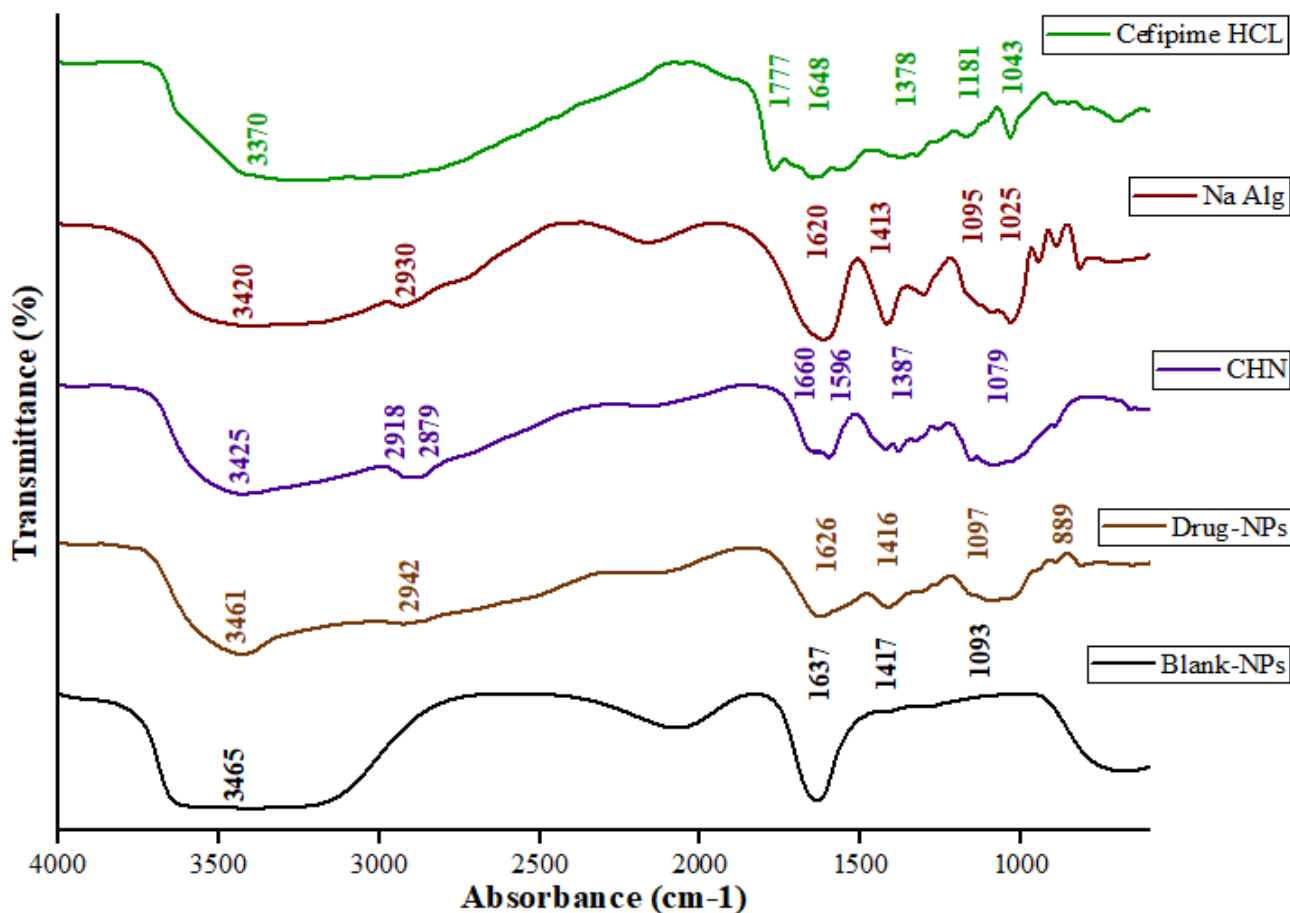
Figure 15. FTIR analysis of blank chitosan NPs, drug loaded chitosan NPs, pure chitosan, sodium alginate and cefepime HCL drug to examine functional groups of each and the changes that were made in NPs after polymers interaction.

In the context of pure chitosan, alginate, cefepime and cefepime-loaded chitosan–alginate nanoparticles, there was a slight change in the peak absorbance of various chemical groups, like amino groups, carboxyl groups, secondary amine groups, and the stretching vibrations of amines and hydroxyls after they formed complexes. These findings recommend that the carboxylate group in alginate effectively interacted with the protonated chitosan amino group due to electrostatic attraction. Furthermore, in the cefepime-loaded chitosan–alginate nanoparticles compared with blank CHN-Alg NPs, there were minor shifts in the alcoholic hydroxyl stretch and the symmetric hydrocarbons band, indicating the presence of an interaction between the nanoparticle complexes and cefepime. Additionally, the presence of small peaks Drug-loaded NPs as opposed to blank-NPs may reflect the physical encapsulation of CEF into CHN-Alg-NPs.

48

4.4. Powdered XRD (pXRD) evaluation

The XRD diffractogram of pure powdered forms of sodium alginate (Na-Alg), Chitosan (CHN), cefepime HCL (Drug), and the blank and drug loaded CHN/Na-Alg nanoparticles is shown in fig (16). The formation of two crystalline peaks at diffraction-angle (2θ) of 13.6^o, and 21.56^o in the X-ray pattern of Na-Alg depicts its semi-crystalline nature. At the same time, the XRD pattern of CHN also reveals its semi-crystallinity behaviour with maximum peaks at $2\theta= 19.8^o$ and 25.4^o (Jana, Trivedi et al. 2015). Furthermore, multiple crystalline peaks are observed in the XRD pattern of pure cefepime at $2\theta= 14.147o, 22.865o, 25o, 28.63o, 30.53o, 32.94o, 35.01o, 41o, 43.56o,$ and $46o$ showing that the drug is crystalline in nature. The blank-CHN/Alg nanoparticles gave two broad peaks with reduced intensity instead of distinct peaks at $2\theta= 30^o\text{-}33.45^o$ and $42^o\text{-}45^o$ indicating an amorphous pattern (Qi, Jiang et al. 2015). After loading of the drug cefepime HCL into CHN/Alg NPs, the intensity of the broad crystalline peak increased at $2\theta=30^o$ as well as decrement of crystalline peak $2\theta=42^o$ depicting that the cefepime is loaded inside the amorphous region of nano-capsules. Reportedly, the amorphous form of a drug is considered more favourable in nanoparticles compared to its crystalline counterpart due to its significantly increased solubility. This characteristic contributes to an extended shelf life and enhances the long-term stability of the drug in aqueous suspensions (Bairwa and Jachak 2016). Additionally, the diffraction peaks that were seen in pure CHN, Na-Alg and the cefepime drug disappeared in cefepime loaded CHN/Alg nano formulation because of the complexation that happened among the drug and CHN/Alg NPs (Hassani, Mahmood et al. 2020).
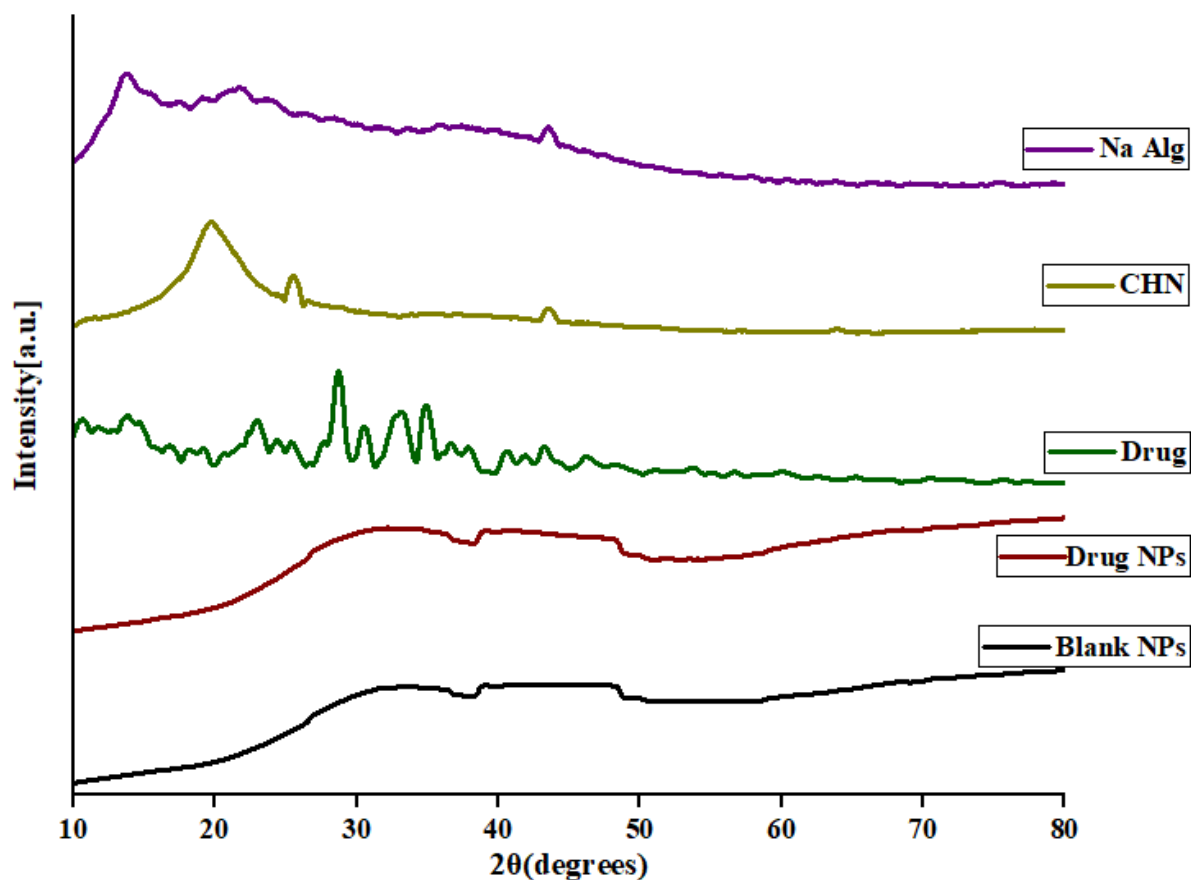
Figure 16. XRD analysis of blank NPs, drug-loaded NPs, pure drug, chitosan, and sodium alginate to analyze the amorphous nature of drug after entrapment into a semi-crystalline chitosan matrix.

4.5. Physical appearance of the gel

The physical properties of the two gel forms were examined visually. Both the commercially available cefepime and the carbopol gel of CEF-CHN-NPs had a uniform, jelly-like texture. CEF-CHN-NPs had a pale, whitish color compared with the commercially available CEF-gel, which had a translucent, colourless appearance.

4.5.1. pH measurement

In this research, we used carbopol 940 as a polymer to make a gel that has an acidic pH in the range of about 3-4. The ideal pH range for carbopol gel is between 4.5 and 6.5 to minimize discomfort and allergic reactions and increase consumer acceptability. As a result, the pH was adjusted to 4–6.5 by adding a few drops of triethanolamine to the carbopol gel dose. Triethanolamine also contributes to the formation of a safe, stable, and high-quality matrix gel and gel base (Safitri, Nawangsari et al. 2021). The pH of the gel was determined to be 5.5±0.55, which is within the range required for topical application.

4.5.2. Spreadability measurement
The effectiveness of treatment through gels is determined based on their spreadability. For the gel to be applied to the skin uniformly, it must be well spreadable and match the ideal parameters for topical application. Furthermore, this is believed to be a critical element in a patient's acceptance of their medication. The spreadability of the CEF-CHN-NPs loaded gel was found to be 4.5cm/1min and 5.5cm/2min, which was considered to have a high spreadability within a short time of spread (Saryanti and Zulfa 2017). Spreadability percentage was calculated as 225±2.309% and 275±0.577% (Kazim, Tariq et al. 2021).

4.5.3. Viscosity measurement
The gel is anticipated to exhibit a viscosity like that of an ointment, with the intention of prolonging its contact time with the skin compared to typical gels. Moreover, the desired viscosity level also seeks to minimize the water content within the gel. This is essential because a lower water content can potentially inhibit microbial growth when the gel is applied to injured skin. There is also concern that a high-water content may impede the clotting process of blood, as it could make the skin excessively moist. The results have shown that the viscosity of NP-loaded carbopol ranged from 28055±19.0087 to 60943±3.05505cps and the viscosity of marketed drug loaded gel ranged from 26234±3.5118 cps to 5303±4.582576 cps.

4.5.4. Drug content
Determination of 96% of drug content from the CEF-CHN-NPs loaded gel is indicating that the drug cefepime was distributed uniformly in the carbopol gel and much less drug loss was happened during the preparation of CEF-CHN-NPs loaded gel.

4.6. Evaluation of the in vitro release study
Figure 17 shows the in vitro cumulative drug release profile of CEF from CEF-CHN-NPs with a CEF-CHN-NPs loaded gel in comparison to free CEF. The data clearly demonstrate the CEF quick release nature, with over 89.93% of the medication released in under 4 hours. On the other hand, CEF showed a 24-h continuous release pattern from both the carbopol gel and the studied nanoparticles. The controlled release of the integrated drug from the nanoparticle core appears to be caused by the strong association between CEF and the CHN that may have resulted from intermolecular hydrogen interactions, as seen by the slow-release profile of CEF from NPs. The release profile of cefepime from the NPs was determined to be approximately 74.44%, which is more than that of the corresponding carbopol gel i.e., 65.33%. Gel exhibited a delayed

51

CEF release compared with NPs because of the presence of an obstacle of the additional carbopol gel matrix. Because a delayed release keeps the therapeutic concentration stable for an extended time span and a fast release boosts penetration, the gradual release of CEF from the corresponding gel facilitate topical administration (Siafaka, Özcan Bülbül et al. 2023).
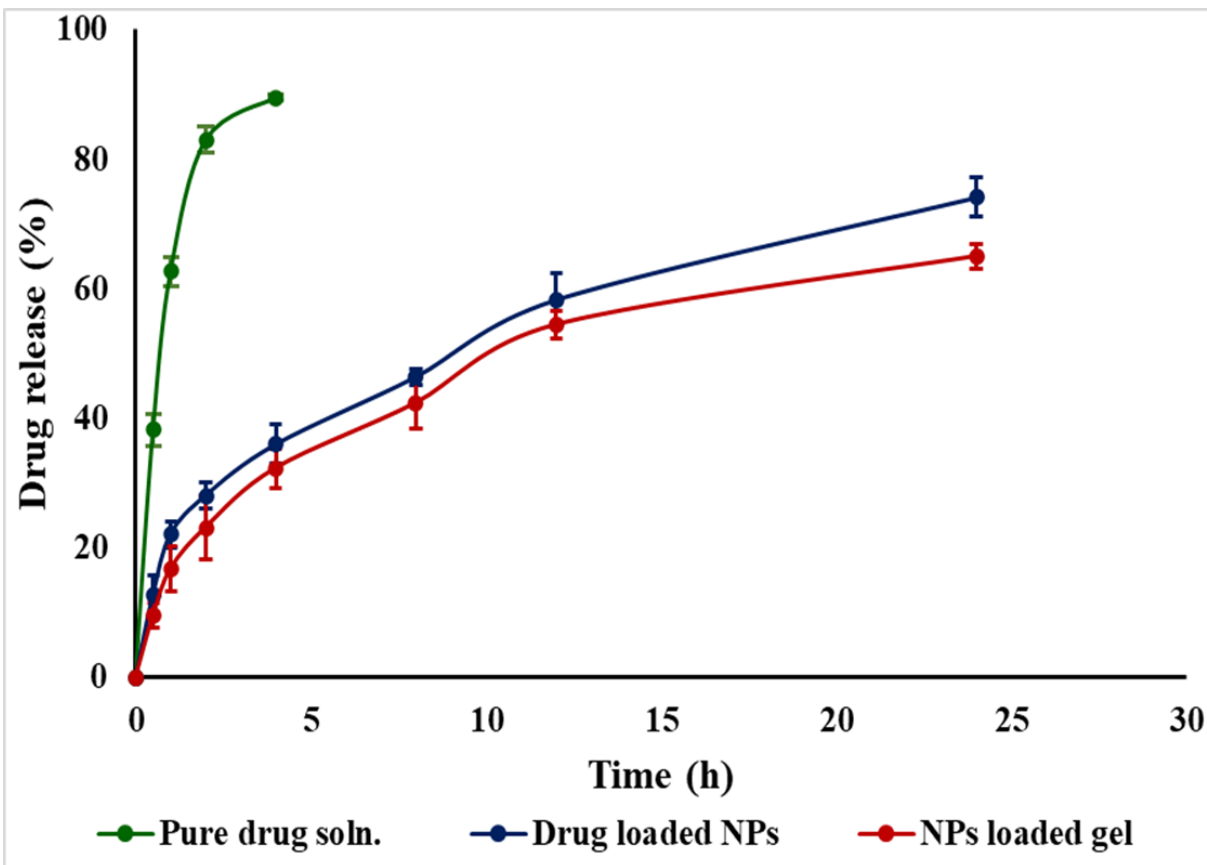
Figure 17. Cumulative drug release profile of pure cefepime, cefepime nanoparticles and cefepime nanoparticle-loaded carbopol gel

Fig (18) reveals the release profile of cefepime from both NPs and gel over a period of 24 h at two different pH (5.5 and 7.4). The release profiles indicate that the release of CEF from the NPs over a 24-h period was slower at pH 7.4 compared to pH 5.5. Specifically, 74.44% of the NPs were released at pH 5.5, while only 50.25% was released at pH 7.4 within the same timeframe.
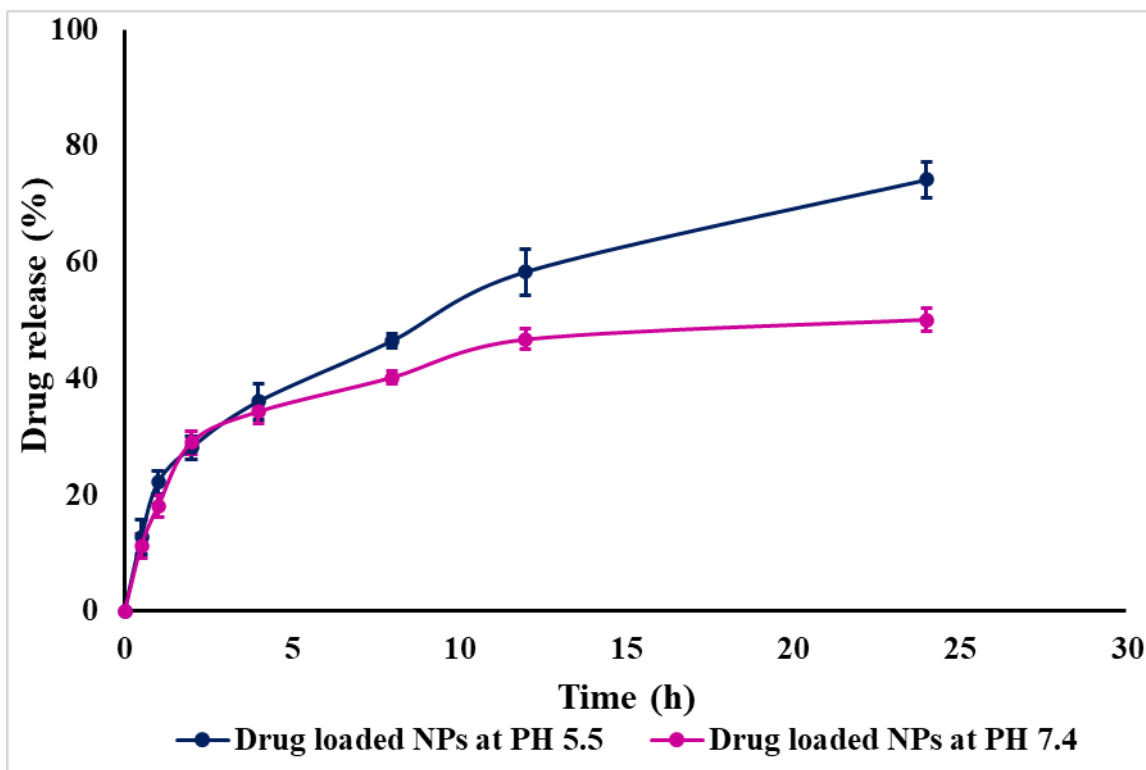
Figure 18. Drug release profile of cefepime nanoparticles at two different pH (7.4 and 5.5)

This indicate that the release of CEF from the NPs is more rapid under acidic conditions. This accelerated release may be attributed to the enhanced swelling capacity of chitosan at acidic (5.5) pH levels (Aydin and Pulat 2012, Mirnejad, Mofazzal Jahromi et al. 2014).

4.7. Drug release kinetics

The researchers extensively elucidate the drug release mechanisms from nanoparticles, which typically involve desorption, diffusion, and matrix degradation. Recent studies have shifted their focus towards biopolymers that respond to physiological variations, such as pH, temperature, and external stimuli, enabling controlled release of therapeutic agents. Different kinetic models were used to analyze the drug release data of free drug, drug-loaded nanoparticles, and corresponding carbopol gel to anticipate drug release processes at different pH levels. subsequently, DD Solver 1.0 was used to study the kinetics of in vitro drug release. A variety of kinetic models, such as Higuchi, Korsmeyer–Peppas, zero order, first order, and Hixson Crowell, provide unique insights into the pharmacokinetics of drug release in the release medium (Saqib, Ali Bhatti et al. 2020). The kinetic models were utilized to evaluate the in vitro drug release strategy in a particular polymeric system. The coefficient of determination (R-squared), which has values ranging from

0 to 1, is used as a measure of the linear regression models' goodness of fit. In vitro release tests for gel and nanoparticles (NPs) were carried out in this work at pH values of 5.5 and 7.4. Beneficial relationships between the medication and the release medium were observed in these trials. The analysis of data using the kinetic models revealed that the drug release from each system adhered closely to the Korsmeyer–Peppas model, as indicated by a high R-squared value, as presented in the Table (4). The diffusion exponent (n), also known as the release exponent (n), was determined to be 0.408 and 0.430 for both NPS as well as gel, as presented in Table 3. A value of n less than 0.5 indicates that the drug release follows a Fickian diffusion transport mechanism, signifying a strong fitness of the data. Furthermore, less R^2 value of the Hixson-Crowell model implies that surface area does not change with time and may also support the idea that the change is dependent on release mechanisms generated by stimuli.

Table 4. Depicting the R2 values of different models for drug release mechanism

	Zero-order	First-order	Higuchi's model	Hixson-Crowell's	Korsmeyer's-Peppas's	
	Correlation value (R^2)	Correlation value (R^2)	Correlation value (R^2)	Correlation value (R^2)	Correlation value (R^2)	n-value
Free CEF soln.	0.49	0.9688	0.9581	0.9291	0.9954	0.356
CEF-CHN-NPs	0.5130	0.8428	0.9734	0.7739	0.9952	0.408
CEF-CHN-NPS-loaded gel	0.5595	0.8416	0.9774	0.7724	0.9896	0.430

4.8. Antibacterial assessment of cefepime nanoparticle carbopol gel

An agar well diffusion assay has been employed to compare the overall antibacterial activity of cefepime and the increased effectiveness in antibacterial activity brought about by the preparation of optimized cefepime nanoparticles by measuring the size of the inhibition zones as depicted in fig (19). Both the pure medication, cefepime used as a positive control, and the

cefepime chitosan nanoparticles (P7) demonstrated a notable zone of inhibition against E. coli and S. aureus. In contrast, no inhibition zone was observed by the blank-CHN-NPs. Comparing the optimized CEF-CHN-NPs to pure cefepime medication dissolved in water, the NPs exhibited a greater zone of bactericidal activity against strains of both E. coli and S. aureus confirming that nanoparticulate system enhances the drug permeation, leading to robust antibacterial response. The diameters of the inhibition zones of each against both strains are presented by a bar graph (19(a)). The possible mechanism involves depolarization that results from polycationic nano-matrix adsorption to the negatively charged bacterial cell membrane, making it easier to penetrate. The bacterial wall would deteriorate and become hazy, resulting in cytoplasm material leakage affecting cell viability. This feature is observed in both Gram-positive and Gram-negative species (Tamara, Lin et al. 2018, Ullah, Javed et al. 2019).
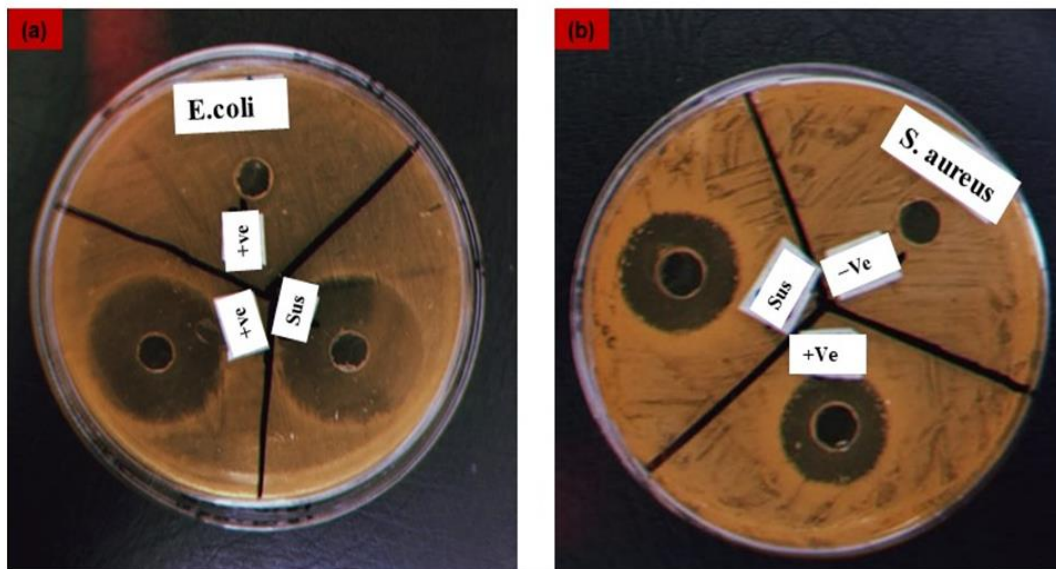
Figure 19. Antibacterial activity of the optimized CEF-CHN-NPs compared with that of the pure Cefepime solution.
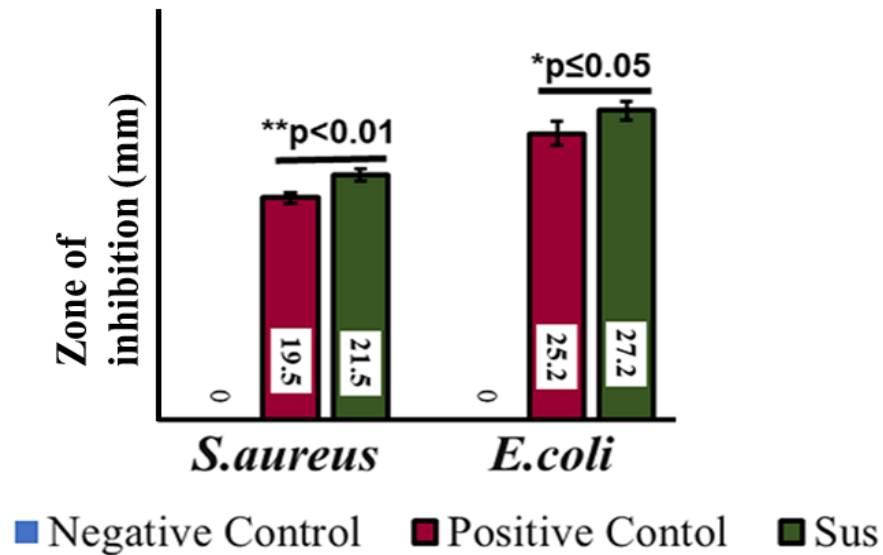
Figure 19. (a) Bar graph showing the inhibition zones (mm) formed by the optimized nano-formulation against gram-positive and gram-negative bacterial strains.

On the other hand, fig (20) demonstrated the antibacterial activity of CEF-CHN-NPs loaded carbopol gel in comparison to the pure CEF-carbopol gel (positive control) against E. coli, K. pneumonia (negative bacterial strain) and S. aureus (positive bacterial strain). Although both the NPs loaded gel and drug loaded gel exhibit significant zone of inhibition, but NPs loaded gel reveals a prominent zone with a diameter of approximately 23.5±0.5mm and 35.2±0.3mm against S. aureus and E. coli respectively. The zone formed by the NPs loaded gel against K. pneumonia is 13.5±0.6mm in comparison to the pure drug gel having no inhibition zone, as illustrated in table along with the bar graph (20(a)). This suggest that K. pneumonia is resistant to cefepime drug (Jamil, Habib et al. 2016), but CEF-CHN-NPs loaded carbopol gel is somewhat effective because of synergistic effect of cefepime nanoparticles as well as the carbopol gel which is having antibacterial activity.
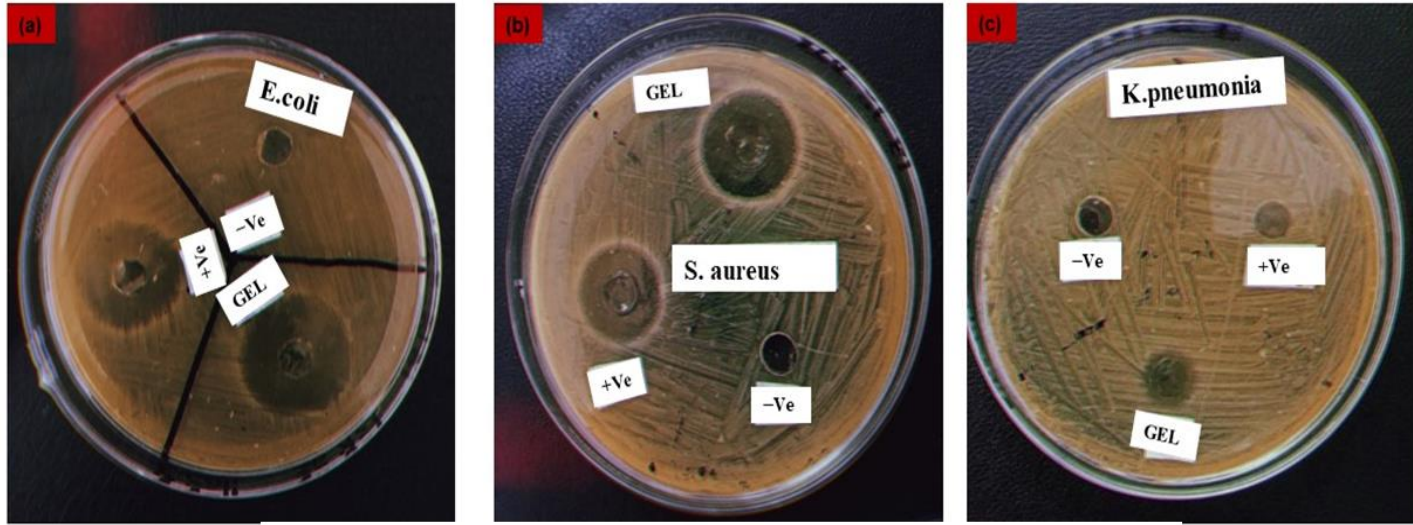
Figure 20. Antibacterial activity of the optimized CEF-CHN-NP- loaded carbopol gel in comparison to the pure CEF-CHN-gel.
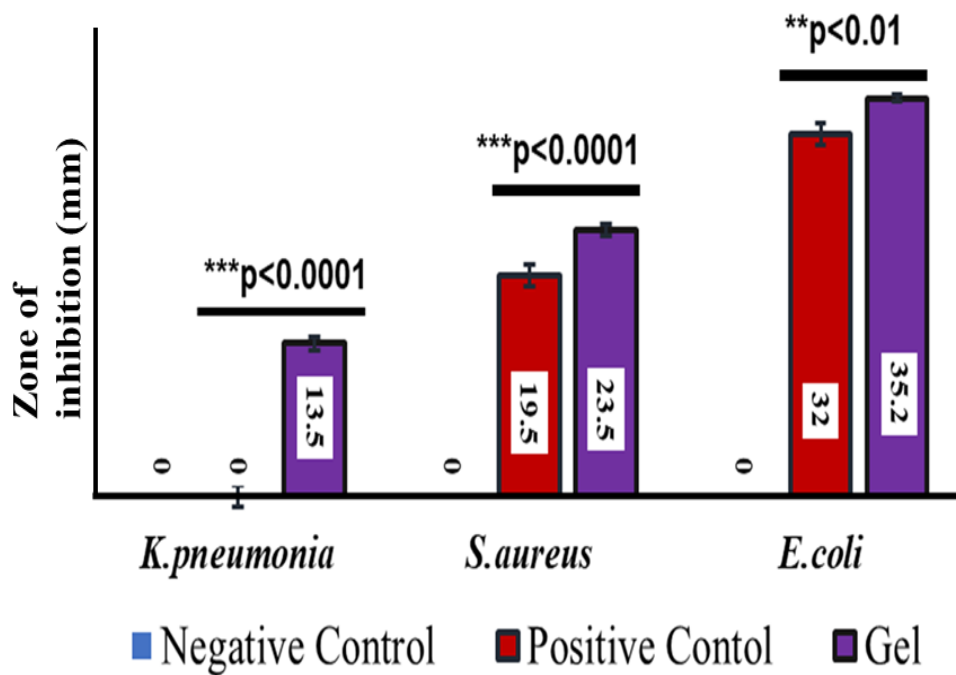
Figure _20_. (a) Bar graph representing the inhibition zones (mm) formed by the gels against different gram-positive and gram-negative bacterial strains.

Furthermore, Variations in cell wall structure and membrane permeability contribute to distinct responses of both gram-positive and gram-negative bacterial strains when exposed to Cefepime-loaded Chitosan nanoparticles (CEF-NPs) and CEF-NPs Carbopol gel, as depicted in bar graphs in fig (19,20) (Kim, Kuk et al. 2007).

CHAPTER 5. DISCUSSION

Advanced medical research is experiencing challenges due to the worldwide prevalence of resistance to multiple medications (Magiorakos, Srinivasan et al. 2012). Cephalosporins, also referred as antibiotics with beta-lactam structure, are prescribed for the treatment of a variety of illnesses brought on by both gram-positive and gram-negative bacteria. The five generations of cephalosporins can be used to treat numerous infectious diseases, including meningitis, resistant bacteria, skin infections, and other conditions (Bui and Preuss 2023). Cefepime, a broad-spectrum antibacterial drug, is a class of 4th generation of cephalosporins that is having the ability of bactericidal activity against both Gram-positive and Gram-negative bacterial strains (Okamoto, Nakahiro et al. 1994). However, the overuse and inappropriate administration of antibacterial medications is the primary cause of antimicrobial resistance in microorganisms (van der Bij and Pitout 2012). Unfortunately, the rates of resistance by fourth generation cephalosporins(cefepime) against E. coli as well as s. aureus are rising swiftly (Collignon 2009). Therefore, in this advanced era, polymeric nanoparticles are often used as smart polymer in light of their declined toxicities and enhanced target specificity (Nejati-Koshki, Mesgari et al. 2014).

Using eight distinct formulations, the relationship between particle size zeta potential and entrapment efficiency has been examined. Every prepared formulation was nanoscale in size. The formulations' mean particle size (effective diameter) ranged widely, from 230.05±0.0 nm to 721±0.0 nm. Table 1 displays the particle size, zeta-potential values and entrapment efficiencies for various formulations. The most crucial elements in regulating the size and stability of the experiments we conducted were the selection of an appropriate stabilizer and its concentration; tween-80 was employed at a different concentration (Table 2). Zeta potential values for eight preparations are shown in fig (10) that ranges from +9.05-18mV. The results of zeta potential i.e., +18mV as shown in fig (11) of the optimized formulation illustrated the positive charge on the surface of the nanoparticulate matrix that is formed by positively charged chitosan polymer (Talib, Ahmed et al. 2021). The value of zeta-potential i.e., 18 demonstrating the physical stability of the suspension because of large number of equally charged particles, manifesting more electrostatic repulsion between them (Sumathi, Tamizharasi et al. 2017). To analyze the surface morphology of the nanoparticles, SEM study was implemented. Smooth surface was observed with spherical morphology of nanoparticles shown in fig (14). Hence, cross linking of

chitosan polymer with the sodium alginate along with the surfactant tween-80 produced better surface properties. Nanosized particles in SEM results are in agreement with those obtained by particles size distribution (Talib, Ahmed et al. 2021). The percentage of entrapment efficiency of all preparations were calculated by making a calibration curve, formulating a linear regression equation (Y= mx+c) shown in fig (13). The drug encapsulation efficiency of P7(optimized formulation) was high when compared to the other preparations. High entrapment efficiency is because of the optimized polymer concentration. One more crucial factor that is responsible for improved entrapment of drug is surfactant concentration that agrees with another study (Patil and Bhoskar 2014).

For the evaluation of functional groups as well as the chemical stability of the entrapped drug inside the nano-preparation, FT-IR technique was performed. After observing the FT-IR results of pure chitosan, sodium alginate, cefepime HCL, blank and drug laded chitosan-alginate nanoparticles as presented in fig (15), the successful crosslinking of chitosan and sodium alginate is confirmed (NH2 bending peak at 1596cm-1). The presence of distinctive bands in free as well as drug loaded chitosan nanoparticles (-COO-, CH2) bands but with shifting and stretching of these bands manifests the chemical stability of nano-preparations (Sahu, Mallick et al. 2010, Patil and Bhoskar 2014). Furthermore, to evaluate the physical nature of the drug-loaded nanoparticles, a technique of powdered X-ray diffraction was employed. XRD-pattern of sodium alginate (Na-Alg), Chitosan (CHN), cefepime HCL (Drug), and the blank and drug loaded CHN/Na-Alg nanoparticles were shown in fig (16). The multiple characteristic-peaks of pure cefepime HCL have shown the crystallinity nature of drug. However, drug-loaded cefepime nanoparticles have not shown any characteristic peak, instead a broad-band with less intensity was observed indicating that drug loaded nano-preparation is in amorphous or disordered crystalline phase (Mahapatra and Murthy 2014).

After the characterization of optimized cefepime loaded chitosan nanoparticles, cefepime nanoparticles loaded carbopol gel was formulated with the gel like consistency. Further characterization of the gel was studied for its safety and patient compliance involving gel physical appearance, pH testing, gel spread ability, and drug content etc. pH measurement was done to obtain an ideal pH for skin infections to minimize discomfort and allergic reactions. The obtained pH was 5.5±0.05, suitable for topical release of drug (Safitri, Nawangsari et al. 2021).

The spreadability of cefepime nanoparticles loaded carbopol gel for topical drug release was found to be 4.5cm/1min and 5.5cm/2min, considered to be high spread within short time duration (Saryanti and Zulfa 2017). The viscosity of cefepime nanoparticles loaded gel was found to be 28055±19.0087 to 60943±3.05505cps with respect to different RPM that is higher than the marketed gel (Maqsood, Masood et al. 2015). The viscosity of the gel must be higher to prolong its contact time with the skin in comparison with the conventional gel.

After characterization of the NPs as well as the gel, nano formulations and nanoparticles loaded carbopol gel were investigated for improved drug release as well as antibacterial assays. Drug release profile of free drug solution. Cefepime loaded nanoparticles and cefepime nanoparticles loaded gel at pH of skin (5.5) is shown in fig (17). It was seen that 89.93% of free drug solution was released within four hours, while 74.44% of the nanoformulation was released within the duration of 24h expressing sustained release. In contrast to nanosuspension, drug loaded carbopol gel has shown the drug release percent as 65.33% manifesting the sustained release. The gradual release of CEF from the corresponding gel facilitates topical administration because the slower release maintains the therapeutic concentration stable for a longer period of time and a fast release increases penetration (Siafaka, Özcan Bülbül et al. 2023).

Antibacterial assays of cefepime nanoparticles as well as cefepime nanoparticles loaded gel in comparison to pure drug solution and pure drug gel were investigated against both positive and negative bacterial strains separately as shown in fig (19). Nanoparticles have shown greater zone of inhibition for both E. coli and S.aureus in comparison to pure drug solution as depicted in bar graphs with significance value as ($p < 0.05$). This is because of the depolarization that happens from polycationic chitosan nano matrix adsorption to the negatively charged bacterial cell membrane, facilitating NPs penetration into the bacterial cytoplasm (Tamara, Lin et al. 2018, Ullah, Javed et al. 2019). Furthermore, it was found that the nanoparticles loaded carbopol gel has shown bactericidal activity against K.pneumonia that is resistant to cefepime drug with 13.5±0.6mm in comparison to the marketed cefepime gel.

6. Conclusions

Over the course of this study, the application of various physical characterization approaches has been instrumental in furnishing substantial data regarding the effectiveness of the synthesis strategy utilized in the generation of chitosan nanoparticles that contain medications like cefepime HCL. Biodegradable nanoparticles loaded with antibiotics play a crucial role in managing infectious diseases such as skin infections, offering a means to enhance therapeutic efficacy while preventing antibiotic overdosing. Successful preparation of cefepime, a bactericidal agent, was achieved in the form of chitosan nanoparticles embedded in carbopol gel, exhibiting desired characteristics. In vitro release studies revealed sustained drug release over 24 hours from the optimized formulations, demonstrating its potential for prolonged therapeutic impact. This study demonstrates that cefepime nanoparticles loaded in carbopol gel present a promising alternative to conventional approaches, enabling targeted drug delivery to the site of action, minimizing off-target effects and improving the overall therapeutic precision. This offers an efficient administration strategy for non-compliant patients. Moreover, Evaluation of antifouling activity against both Gram-positive strain(*S.aureus*) and Gram-negative strain (*E.coli, K.pneumonia*) by the nanoformulation as well the gel has shown better zones of inhibition depicting their enhanced bactericidal activity than conventional drug. These results offer insights into their possible effectiveness in situations wherein resistance problems may limit the use of conventional medications. In short, the continual pursuit of novel and enhanced therapies for diseases that must have a potent activity and be cost-effective through nanomedicine is creating a substantial need for scientific research.

7. Future Perspectives

The proposed research aims to establish and characterise chitosan nanoparticles in order to optimise the production of cefepime-loaded nanoparticles, which will subsequently be transformed into carbopol gel for improved skin treatment efficacy. There is an opportunity that the findings from this study will open up innovative, and interesting research directions. The results of this investigation will greatly advance our knowledge of the fundamental mechanisms causing both the therapeutic benefits and potential side effects by taking a comprehensive strategy. As a result, this will help in the creation of better and more informed approaches to therapy. As a whole, the research's future prospects demand for an all-encompassing approach that necessitate a number of dimensions. Such dimensions include additional research employing

animal models to improve the accuracy and validity of the results e.g., skin irritation studies as well as skin permeation analysis. To increase the range of possible treatment options, research into substitute polymers can also be conducted. In order to obtain an in-depth comprehending of the procedures being performed, a final step will be a thorough examination of the molecular complexities underlying skin management. The application of chitosan nanoparticles has surfaced as a possible revolutionary approach towards augmenting the efficacy and specificity of anti-bacterial drugs.

-

REFERENCES

Abdelghany, S., et al. (2017). "Carrageenan-stabilized chitosan alginate nanoparticles loaded with ethionamide for the treatment of tuberculosis." Journal of Drug Delivery Science and Technology **39**: 442-449.

Aderibigbe, B. A. and T. Naki (2018). "Design and efficacy of nanogels formulations for intranasal administration." Molecules **23**(6): 1241.

Agnihotri, S. A., et al. (2004). "Recent advances on chitosan-based micro-and nanoparticles in drug delivery." Journal of controlled release **100**(1): 5-28.

Ahad, A., et al. (2017). "Pharmacodynamic study of eprosartan mesylate-loaded transfersomes Carbopol® gel under Dermaroller® on rats with methyl prednisolone acetate-induced hypertension." Biomedicine & Pharmacotherapy **89**: 177-184.

Ahmad, R. M., et al. (2022). "Preparation and Characterization of Blank and Nerolidol-Loaded Chitosan–Alginate Nanoparticles." Nanomaterials **12**(7): 1183.

Ahmed, N., et al. (2013). "Polymeric drug delivery systems for encapsulating hydrophobic drugs." Drug Delivery Strategies for Poorly Water-Soluble Drugs: 151-197.

Akhtar, M., et al. (2015). "Biosynthesis and characterization of silver nanoparticles from methanol leaf extract of Cassia didymobotyra and assessment of their antioxidant and antibacterial activities." Journal of Nanoscience and Nanotechnology **15**(12): 9818-9823.

Al-Hamadani, M. H. and S. Al-Edresi (2022). "Formulation and Characterization of Hydrogel of Proniosomes Loaded Diclofenac Sodium."

Appa, A. A., et al. (2017). Characterizing cefepime neurotoxicity: a systematic review. Open forum infectious diseases, Oxford University Press US.

Avadi, M. R., et al. (2010). "Preparation and characterization of insulin nanoparticles using chitosan and Arabic gum with ionic gelation method." Nanomedicine: Nanotechnology, Biology and Medicine **6**(1): 58-63.

Aydin, R. S. T. and M. Pulat (2012). "5-Fluorouracil encapsulated chitosan nanoparticles for pH-stimulated drug delivery: evaluation of controlled release kinetics." Journal of Nanomaterials **2012**: 42-42.

Azhdarzadeh, M., et al. (2012). "Anti-bacterial performance of azithromycin nanoparticles as colloidal drug delivery system against different gram-negative and gram-positive bacteria." Advanced pharmaceutical bulletin **2**(1): 17.

Bairwa, K. and S. M. Jachak (2016). "Nanoparticle formulation of 11-keto-β-boswellic acid (KBA): Anti-inflammatory activity and in vivo pharmacokinetics." Pharmaceutical Biology **54**(12): 2909-2916.

Balouiri, M., et al. (2016). "Methods for in vitro evaluating antimicrobial activity: A review." Journal of pharmaceutical analysis **6**(2): 71-79.

Balya, H., et al. (2021). "Fabrication of novel bio-compatible cefixime nanoparticles using chitosan and Azadirachta indica fruit mucilage as natural polymers." Journal of Drug Delivery Science and Technology **66**: 102750.

Banerjee, M., et al. (2010). "Heightened reactive oxygen species generation in the antimicrobial activity of a three component iodinated chitosan– silver nanoparticle composite." Langmuir **26**(8): 5901-5908.

Bauer, K. A., et al. (2013). "Extended-infusion cefepime reduces mortality in patients with Pseudomonas aeruginosa infections." Antimicrobial Agents and Chemotherapy **57**(7): 2907-2912.

Berthold, A., et al. (1996). "Preparation and characterization of chitosan microspheres as drug carrier for prednisolone sodium phosphate as model for anti-inflammatory drugs." Journal of Controlled Release **39**(1): 17-25.

Binesh, N., et al. (2021). "Enhanced stability of salt-assisted sodium ceftriaxone-loaded chitosan nanoparticles: Formulation and optimization by 32-full factorial design and antibacterial effect study against aerobic and anaerobic bacteria." Colloids and Surfaces A: Physicochemical and Engineering Aspects **618**: 126429.

Blecher, K., et al. (2011). "The growing role of nanotechnology in combating infectious disease." Virulence **2**(5): 395-401.

Bui, T. and C. V. Preuss (2023). Cephalosporins. StatPearls [Internet], StatPearls Publishing.

ÇAĞLAR, E. Ş., et al. "PREPARATION AND CHARACTERIZATION OF CARBOPOL BASED HYDROGELS CONTAINING DEXPANTHENOL." Journal of Faculty of Pharmacy of Ankara University **47**(3): 6-6.

Chapman, T. M. and C. M. Perry (2003). "Cefepime: a review of its use in the management of hospitalized patients with pneumonia." American Journal of Respiratory Medicine **2**(1): 75-107.

Coates, J. (2000). Interpretation of infrared spectra, a practical approach.

Collignon, P. (2009). Resistant Escherichia coli—we are what we eat, The University of Chicago Press. **49:** 202-204.

Cunha-Azevedo, E. P., et al. (2011). "In vitro antifungal activity and toxicity of itraconazole in DMSA-PLGA nanoparticles." Journal of nanoscience and nanotechnology **11**(3): 2308-2314.

de la Fuente, M., et al. (2010). "Chitosan-based nanostructures: a delivery platform for ocular therapeutics." Advanced drug delivery reviews **62**(1): 100-117.

Deshayes, S., et al. (2017). "Neurological adverse effects attributable to β-lactam antibiotics: a literature review." Drug safety **40**: 1171-1198.

Diseases, N. C. f. I. "Achievements in Public Health, 1900-1999: Control of Infectious Diseases."

Domínguez-Delgado, C. L., et al. (2011). "Preparation and characterization of triclosan nanoparticles intended to be used for the treatment of acne." European journal of pharmaceutics and biopharmaceutics **79**(1): 102-107.

Duceac, L. D., et al. (2020). "Third-generation cephalosporin-loaded chitosan used to limit microorganisms resistance." Materials **13**(21): 4792.

Duceac, L. D., et al. (2019). "Antibiotic molecules involved in increasing microbial resistance." age **5**: 0.01.

Duceac, L. D., et al. (2019). "Synthesis and Characterization of Carbapenem Based Nanohybrids as Antimicrobial Agents for Multidrug Resistant Bacteria." Mater. Plast **56**: 388-391.

Eko, K. E., et al. (2015). "Molecular characterization of methicillin-resistant Staphylococcus aureus (MRSA) nasal colonization and infection isolates in a Veterans Affairs hospital." Antimicrobial resistance and infection control **4**(1): 1-7.

El-Enin, A. S. M. A., et al. (2019). "Proniosomal gel-mediated topical delivery of fluconazole: Development, in vitro characterization, and microbiological evaluation." Journal of Advanced Pharmaceutical Technology & Research **10**(1): 20.

Elsayed, M. M., et al. (2007). "Lipid vesicles for skin delivery of drugs: reviewing three decades of research." International journal of pharmaceutics **332**(1-2): 1-16.

Erbacher, P., et al. (1998). "Chitosan-based vector/DNA complexes for gene delivery: biophysical characteristics and transfection ability." Pharmaceutical research **15**: 1332-1339.

Fan, L., et al. (2008). "Novel super pH-sensitive nanoparticles responsive to tumor extracellular pH." Carbohydrate Polymers **73**(3): 390-400.

Ferdous, S., et al. (2015). "In vitro and in vivo studies of drug-drug interaction between metformin and cefepime." Pharm Anal Acta **6**(3): 348.

Fung-Tomc, J., et al. (1989). "Activity of cefepime against ceftazidime-and cefotaxime-resistant gram-negative bacteria and its relationship to beta-lactamase levels." Antimicrobial Agents and Chemotherapy **33**(4): 498-502.

George, A., et al. (2019). "Natural biodegradable polymers based nano-formulations for drug delivery: A review." International journal of pharmaceutics **561**: 244-264.

Giamarellou, H. (1993). "Low-dosage cefepime as treatment for serious bacterial infections." Journal of Antimicrobial Chemotherapy **32**(suppl_B): 123-132.

Giamarellou, H. (1996). "Clinical experience with the fourth generation cephalosporins." Journal of Chemotherapy (Florence, Italy) **8**: 91-104.

Gonelimali, F. D., et al. (2018). "Antimicrobial properties and mechanism of action of some plant extracts against food pathogens and spoilage microorganisms." Frontiers in microbiology **9**: 1639.

Grenha, A. (2012). "Chitosan nanoparticles: a survey of preparation methods." Journal of drug targeting **20**(4): 291-300.

Gul, R., et al. (2018). "Biodegradable ingredient-based emulgel loaded with ketoprofen nanoparticles." AAPS pharmscitech **19**: 1869-1881.

Guo, W.-Q., et al. (2009). "Optimization of culture conditions for hydrogen production by Ethanoligenens harbinense B49 using response surface methodology." Bioresource technology **100**(3): 1192-1196.

Gutowski, I. A. (2010). "The effects of pH and concentration on the rheology of Carbopol gels."

Hajipour, M. J., et al. (2012). "Antibacterial properties of nanoparticles." Trends in biotechnology **30**(10): 499-511.

Hassan, M. A., et al. (2012). "Antibiotics as microbial secondary metabolites: Production and application." J Sci Eng 2012; 59 (1): 101 **111**.

Hassan, S.-u. and X. Zhang (2019). "Droplet-based microgels: Attractive materials for drug delivery systems." Res. Dev. Mater. Sci **11**: 1183-1185.

Hassani, A., et al. (2020). "Formulation, characterization and biological activity screening of sodium alginate-gum arabic nanoparticles loaded with curcumin." Molecules **25**(9): 2244.

Huwyler, T., et al. (2017). "Cefepime plasma concentrations and clinical toxicity: a retrospective cohort study." Clinical Microbiology and Infection **23**(7): 454-459.

Ichim, D. L., et al. (2019). "Synthesis and characterization of colistin loaded nanoparticles used to combat multi-drug resistant microorganisms." Rev. Chim **70**(10).

Iftikhar, S. Y., et al. (2020). "Desirability combined response surface methodology approach for optimization of prednisolone acetate loaded chitosan nanoparticles and in-vitro assessment." Materials Research Express **7**(11): 115004.

Imam, S. S., et al. (2023). "Formulation of Miconazole-Loaded Chitosan–Carbopol Vesicular Gel: Optimization to In Vitro Characterization, Irritation, and Antifungal Assessment." Pharmaceutics **15**(2): 581.

Isitan, C., et al. (2017). "Cefepime induced neurotoxicity: A case series and review of the literature." Eneurologicalsci **8**: 40-43.

Jamil, B., et al. (2016). "Development of cefotaxime impregnated chitosan as nano-antibiotics: De novo strategy to combat biofilm forming multi-drug resistant pathogens." Frontiers in microbiology **7**: 330.

Jana, S., et al. (2015). "Characterization of physicochemical and thermal properties of chitosan and sodium alginate after biofield treatment." Pharmaceutica Analytica Acta **6**(10).

Jeevanandam, J., et al. (2018). "Review on nanoparticles and nanostructured materials: history, sources, toxicity and regulations." Beilstein journal of nanotechnology **9**(1): 1050-1074.

Kazim, T., et al. (2021). "Chitosan hydrogel for topical delivery of ebastine loaded solid lipid nanoparticles for alleviation of allergic contact dermatitis." RSC advances **11**(59): 37413-37425.

Kessler, R., et al. (1985). "Comparison of a new cephalosporin, BMY 28142, with other broad-spectrum beta-lactam antibiotics." Antimicrobial Agents and Chemotherapy **27**(2): 207-216.

Kessler, R. E. (2001). "Cefepime microbiologic profile and update." The Pediatric infectious disease journal **20**(3): 331-336.

Kim, J. S., et al. (2007). "Antimicrobial effects of silver nanoparticles." <u>Nanomedicine: Nanotechnology, biology and medicine</u> **3**(1): 95-101.

Kong, M., et al. (2010). "Antimicrobial properties of chitosan and mode of action: a state of the art review." <u>International journal of food microbiology</u> **144**(1): 51-63.

Kumar, A., et al. (2011). "Preparation, characterization, and in vitro antimicrobial assessment of nanocarrier based formulation of nadifloxacin for acne treatment." <u>Die Pharmazie-An International Journal of Pharmaceutical Sciences</u> **66**(2): 111-114.

Laxminarayan, R., et al. (2013). "Antibiotic resistance—the need for global solutions." <u>The Lancet infectious diseases</u> **13**(12): 1057-1098.

Lee, S., et al. (2005). "Cationic analog of deoxycholate as an oral delivery carrier for ceftriaxone." <u>Journal of pharmaceutical sciences</u> **94**(11): 2541-2548.

Leso, V., et al. (2019). "Biomedical nanotechnology: Occupational views." <u>Nano Today</u> **24**: 10-14.

Li, P., et al. (2008). "Chitosan-alginate nanoparticles as a novel drug delivery system for nifedipine." <u>International journal of biomedical science: IJBS</u> **4**(3): 221.

Lim, C., et al. (2016). "Epidemiology and burden of multidrug-resistant bacterial infection in a developing country." <u>elife</u> **5**: e18082.

Luca, A. C., et al. (2020). "Drug Encapsulated Nanomaterials as Carriers Used in Cardiology Field." <u>Rev. Chim</u> **71**: 413-417.

Ma, Y., et al. (2008). "Preparation of chitosan–nylon-6 blended membranes containing silver ions as antibacterial materials." <u>Carbohydrate research</u> **343**(2): 230-237.

Magiorakos, A.-P., et al. (2012). "Multidrug-resistant, extensively drug-resistant and pandrug-resistant bacteria: an international expert proposal for interim standard definitions for acquired resistance." <u>Clinical microbiology and infection</u> **18**(3): 268-281.

Mahapatra, A. K. and P. Murthy (2014). "Solubility and dissolution rate enhancement of efavirenz by inclusion complexation and liquid anti-solvent precipitation technique." <u>J Chem Pharm Res</u> **6**(4): 1099-1106.

Maqsood, I., et al. (2015). "Preparation and in vitro evaluation of Nystatin micro emulsion based gel." <u>Pakistan Journal of Pharmaceutical Sciences</u> **28**(5).

Mehta, D. and A. K. Sharma (2016). "Cephalosporins: A review on imperative class of antibiotics." Inventi Rapid: Molecular Pharmacology **1**: 1-6.

Mirnejad, R., et al. (2014). "Curcumin-loaded chitosan tripolyphosphate nanoparticles as a safe, natural and effective antibiotic inhibits the infection of Staphylococcus aureus and Pseudomonas aeruginosa in vivo." Iranian Journal of Biotechnology **12**(3): 1-8.

Mohanambal, E. (2010). Formulation and evaluation of pH triggered in situ gelling system of levofloxacin, Madurai Medical College, Madurai.

Mohsin, M., et al. (2019). "Excessive use of medically important antimicrobials in food animals in Pakistan: a five-year surveillance survey." Global health action **12**(sup1): 1697541.

Mubeen, B., et al. (2021). "Nanotechnology as a novel approach in combating microbes providing an alternative to antibiotics." Antibiotics **10**(12): 1473.

Murray, C. J., et al. (2022). "Global burden of bacterial antimicrobial resistance in 2019: a systematic analysis." The Lancet **399**(10325): 629-655.

Mushtaq, S., et al. (2017). "Biocompatible biodegradable polymeric antibacterial nanoparticles for enhancing the effects of a third-generation cephalosporin against resistant bacteria." Journal of Medical Microbiology **66**(3): 318-327.

Nagpal, K., et al. (2010). "Chitosan nanoparticles: a promising system in novel drug delivery." Chemical and Pharmaceutical Bulletin **58**(11): 1423-1430.

Nejati-Koshki, K., et al. (2014). "Synthesis and in vitro study of cisplatin-loaded Fe3O4 nanoparticles modified with PLGA-PEG6000 copolymers in treatment of lung cancer." Journal of microencapsulation **31**(8): 815-823.

Nguyen, H. M., et al. (2014). "Determining a clinical framework for use of cefepime and β-lactam/β-lactamase inhibitors in the treatment of infections caused by extended-spectrum-β-lactamase-producing Enterobacteriaceae." Journal of Antimicrobial Chemotherapy **69**(4): 871-880.

Nichols, H. (2018). The top 10 leading causes of death in the United States. Medical News Today.

Okamoto, M. P., et al. (1994). "Cefepime: a new fourth-generation cephalosporin." American Journal of Health-System Pharmacy **51**(4): 463-477.

Patel, H. B., et al. (2019). "The role of cefepime in the treatment of extended-spectrum beta-lactamase infections." Journal of Pharmacy Practice **32**(4): 458-463.

Patil, P. and M. Bhoskar (2014). "Optimization and evaluation of spray dried chitosan nanoparticles containing doxorubicin." Int. J. Curr. Pharm. Res **6**(2): 7-15.

Payne, L. E., et al. (2017). "Cefepime-induced neurotoxicity: a systematic review." Critical care **21**(1): 1-8.

Pillai, C. K., et al. (2009). "Chitin and chitosan polymers: Chemistry, solubility and fiber formation." Progress in polymer science **34**(7): 641-678.

Prabaharan, M. and J. Mano (2004). "Chitosan-based particles as controlled drug delivery systems." Drug delivery **12**(1): 41-57.

Prajapati, S. K., et al. (2019). "Biodegradable polymers and constructs: A novel approach in drug delivery." European polymer journal **120**: 109191.

Qi, L., et al. (2004). "Preparation and antibacterial activity of chitosan nanoparticles." Carbohydrate research **339**(16): 2693-2700.

Qi, Y., et al. (2015). "Synthesis of quercetin loaded nanoparticles based on alginate for Pb (II) adsorption in aqueous solution." Nanoscale research letters **10**: 1-9.

Rai, M. K., et al. (2012). "Silver nanoparticles: the powerful nanoweapon against multidrug-resistant bacteria." Journal of applied microbiology **112**(5): 841-852.

Ramkumar, V. S., et al. (2017). "Biofabrication and characterization of silver nanoparticles using aqueous extract of seaweed Enteromorpha compressa and its biomedical properties." Biotechnology reports **14**: 1-7.

Reese, M. (2013). "Nanotechnology: using co-regulation to bring regulation of modern technologies into the 21st century." Health matrix **23**: 537.

Rivera, C. G., et al. (2016). "Impact of cefepime susceptible-dose-dependent MIC for Enterobacteriaceae on reporting and prescribing." Antimicrobial Agents and Chemotherapy **60**(6): 3854-3855.

Rudramurthy, G. R., et al. (2016). "Nanoparticles: alternatives against drug-resistant pathogenic microbes." Molecules **21**(7): 836.

Safitri, F. I., et al. (2021). Overview: Application of carbopol 940 in gel. International Conference on Health and Medical Sciences (AHMS 2020), Atlantis Press.

Sahu, S. K., et al. (2010). "In vitro evaluation of folic acid modified carboxymethyl chitosan nanoparticles loaded with doxorubicin for targeted delivery." Journal of Materials Science: Materials in Medicine **21**: 1587-1597.

Sailaja, A. K., et al. (2011). "Different techniques used for the preparation of nanoparticles using natural polymers and their application." Int J Pharm Pharm Sci **3**(2): 45-50.

Sanpui, P., et al. (2008). "The antibacterial properties of a novel chitosan–Ag-nanoparticle composite." International journal of food microbiology **124**(2): 142-146.

Saqib, M., et al. (2020). "Amphotericin b loaded polymeric nanoparticles for treatment of leishmania infections." Nanomaterials **10**(6): 1152.

Saryanti, D. and I. N. m. Zulfa (2017). "Optimization Carbopol And Glycerol As Basis Of Hand Gel Antiseptics Extract Ethanol Ceremai Leaf (Phyllantus Acidus (L.) Skeels) With Simplex Lattice Design." JPSCR: Journal of Pharmaceutical Science and Clinical Research **2**(1): 35-43.

Shanmugarathinam, A. and A. Puratchikody (2014). "Formulation and characterisation of ritonavir loaded ethylcellulose buoyant microspheres." Journal of Pharmaceutical Sciences and Research **6**(8): 274.

Siafaka, P. I., et al. (2023). "The application of nanogels as efficient drug delivery platforms for dermal/transdermal delivery." Gels **9**(9): 753.

Silva, M. M. d. (2016). The use of nanoparticles as drug delivery systems for topical administration in the eye.

Sumathi, R., et al. (2017). "Formulation and evaluation of polymeric nanosuspension of naringenin." Int J App Pharm **9**(6): 60-70.

Sur, S., et al. (2019). "Recent developments in functionalized polymer nanoparticles for efficient drug delivery system." Nano-Structures & Nano-Objects **20**: 100397.

Swartz, M. (2000). "Cellulitis and subcutaneous tissue infections." Mandell, Douglas, and Bennett's principles and practice of infectious diseases: 1037-1057.

Talib, S., et al. (2021). "Chitosan-chondroitin based artemether loaded nanoparticles for transdermal drug delivery system." Journal of Drug Delivery Science and Technology **61**: 102281.

Tamara, F. R., et al. (2018). "Antibacterial effects of chitosan/cationic peptide nanoparticles." Nanomaterials **8**(2): 88.

Temkin, E., et al. (2018). "Estimating the number of infections caused by antibiotic-resistant Escherichia coli and Klebsiella pneumoniae in 2014: a modelling study." The Lancet Global Health **6**(9): e969-e979.

Thabit, A. K., et al. (2015). "Antimicrobial resistance: impact on clinical and economic outcomes and the need for new antimicrobials." Expert opinion on pharmacotherapy **16**(2): 159-177.

Tibbitt, M. W., et al. (2016). "Emerging frontiers in drug delivery." Journal of the American Chemical Society **138**(3): 704-717.

Tiyaboonchai, W. (2013). "Chitosan nanoparticles: a promising system for drug delivery." Naresuan University Journal: Science and Technology (NUJST) **11**(3): 51-66.

Tong, X., et al. (2020). "Recent advances in natural polymer-based drug delivery systems." Reactive and Functional Polymers **148**: 104501.

Tuli, H. S. (2019). "Synergistic effect of copper nanoparticles and antibiotics to enhance antibacterial potential."

Ullah, F., et al. (2019). "Determining the molecular-weight and interfacial properties of chitosan built nanohydrogel for controlled drug delivery applications." Biointerface Res. Appl. Chem **9**(6): 4452.

van der Bij, A. K. and J. D. Pitout (2012). "The role of international travel in the worldwide spread of multiresistant Enterobacteriaceae." Journal of Antimicrobial Chemotherapy **67**(9): 2090-2100.

Walker, K. J., et al. (2018). "Clinical outcomes of extended-spectrum beta-lactamase-producing Enterobacteriaceae infections with susceptibilities among levofloxacin, cefepime, and carbapenems." Canadian Journal of Infectious Diseases and Medical Microbiology **2018**.

Wang, L., et al. (2017). "The antimicrobial activity of nanoparticles: present situation and prospects for the future." International journal of nanomedicine: 1227-1249.

Wen, C.-H., et al. (2019). "Molecular structures and mechanisms of waterborne biodegradable polyurethane nanoparticles." Computational and Structural Biotechnology Journal **17**: 110-117.

Whitesides, G. M. (2005). "Nanoscience, nanotechnology, and chemistry." Small **1**(2): 172-179.

Wong, I. Y., et al. (2013). "Nanotechnology: emerging tools for biology and medicine." Genes & development **27**(22): 2397-2408.

Wrenn, R. H., et al. (2018). "Extended infusion compared to standard infusion cefepime as empiric treatment of febrile neutropenia." Journal of Oncology Pharmacy Practice **24**(3): 170-175.

Yadav, E., et al. (2021). "Amelioration of full thickness dermal wounds by topical application of biofabricated zinc oxide and iron oxide nano-ointment in albino Wistar rats." Journal of Drug Delivery Science and Technology **66**: 102833.

Yuan, L., et al. (2022). "Nanocarriers for promoting skin delivery of therapeutic agents." Applied Materials Today **27**: 101438.

Zargartalebi, M., et al. (2015). "Enhancement of surfactant flooding performance by the use of silica nanoparticles." Fuel **143**: 21-27.

Zhu, L.-l. and Q. Zhou (2018). "Optimal infusion rate in antimicrobial therapy: explosion of evidence in the last five years." Infection and drug resistance: 1105-1117.